

TECHNICAL DOCUMENTATION

LOCOMOTIVE TRUCK HUNTING MODEL

V. K. Garg
G. C. Martin
P. W. Hartmann
J. G. Tolomei

MATHEMATICAL MODEL
MATHEMATICAL MODEL



**TECHNICAL
DOCUMENTATION**
LOCOMOTIVE
TRUCK HUNTING MODEL

V. K. Garg
G. C. Martin
P. W. Hartmann
J. G. Tolomei

**MATHEMATICAL MODEL
MATHEMATICAL MODEL**

Steering Committee for the Track Train Dynamics Program

Chairman

J. L. Cann
Vice President
Operation and Maintenance
Canadian National Railways

Vice Chairman

W. J. Harris, Jr.
Vice President
Research and Test Department
Association of American Railroads

E. F. Lind
Project Director-Phase I
Track Train Dynamics
Southern Pacific Transportation Co.

M. D. Armstrong

Chairman
Transportation Development Agency
Canadian Ministry of Transport

W. S. Autrey

Chief Engineer
Atchison, Topeka & Santa Fe Railway Co.

M. W. Bellis

Manager
Locomotive Engineering
General Electric Company

M. Ephraim

Chief Engineer
Electro Motive Division
General Motors Corporation

J. G. German

Vice President
Engineering
Missouri Pacific Co.

W. S. Hansen

President
A. Stucki Co.

W. P. Manos

Vice President
Research and Development
Pullman-Standard

R. A. Matthews

Vice President
Railway Progress Institute

R. G. Maughan

Chairman
Railroad Advisory Committee
Transportation Development Agency

D. K. McNear

Vice President
Operations
Southern Pacific Transportation Co.

L. A. Peterson

Director
Office of Rail Safety Research
Federal Railroad Administration

G. E. Reed

Director
Railroad Sales
AMCAR Division
ACF Industries

D. V. Sartore

Chief Engineer Design
Burlington Northern, Inc.

P. S. Settle

President
Railway Maintenance Corporation

W. W. Simpson

Vice President
Engineering
Southern Railway System

W. S. Smith

Vice President and
Director of Transportation
General Mills, Inc.

J. B. Stauffer

Director
Transportation Test Center
Federal Railroad Administration

***R. D. Spence (Chairman)**

President
ConRail

***L. S. Crane (Chairman)**

President and Chief
Administrative Officer
Southern Railway System

***D. Y. Clem (Vice Chairman)**

President
McConway & Torley Corporation

***C. Bruce Ward (Vice Chairman)**

President
Gunderson, Inc.

***Edward J. Ward (Vice Chairman)**

Acting Associate Administrator for
Research and Development
Federal Railroad Administration

***Former members of this committee**

BACKGROUND INFORMATION
on the
TRACK-TRAIN DYNAMICS PROGRAM

The Track-Train Dynamics Program encompasses studies of the dynamic interaction of a train consist with track as affected by operating practices, terrain, and climatic conditions.

Trains cannot move without these dynamic interactions. Such interactions, however, frequently manifest themselves in ways climaxing in undesirable and costly results. While often differing and sometimes necessarily so, previous efforts to reasonably control these dynamic interactions have been reflected in the operating practices of each railroad and in the design and maintenance specifications for track and equipment.

Although the matter of track-train dynamics is by no means a new phenomena, the increase in train lengths, car sizes and loadings has emphasized the need to reduce wherever possible excessive dynamic train action. This, in turn, requires a greater effort to achieve more control over the stability of the train as speeds have increased and railroad operations become more systemized.

The Track-Train Dynamics Program is representative of many new programs in which the railroad industry is pooling its resources for joint study and action.

A major planning effort on track-train dynamics was initiated in July 1971 by the Southern Pacific Transportation Company under contract to the AAR and carried out with AAR staff support. Completed in early 1972, this plan clearly indicated that no individual railroad has both the resources and the incentive to undertake the entire program. Therefore, the AAR was authorized by its Board to proceed with the Track-Train Dynamics Program.

In the same general period, the FRA signaled its interest in vehicle dynamics by development of plans for a major test facility. The design of a track loop for train dynamic testing and the support of related research program were also pursued by the FRA.

In organizing the effort, it was recognized that a substantial body of information and competence on this problem resided in the railroad supply industry and that significant technical and financial resources were available in government.

Through the Railway Progress Institute, the supply industry coordinated its support for this program and has made available men, equipment, data from earlier proprietary studies, and monetary contributions.

Through the FRA, contractor personnel and direct financial resources have been made available.

Through the Transportation Development Agency, the Canadian Government has made a major commitment to work on this problem and to coordinate that work with the United States' effort.

Through the Office de Recherches et D'Essais, the research arm of the Union Internationale des Chemins de Fer, the basis for a full exchange of information with European groups active in this field had been arranged.

The Track-Train Dynamics Program is managed by the Research and Test Department of the Association of American Railroads under the direction of an industry-government steering committee. Railroad members are designated by elected members of the AAR's Operations-Transportation General Committee, supply industry members by the Railway Progress Institute, U. S. Government members by the Federal Railroad Administration, and Canadian Government members by the Transportation Development Agency. Appropriate task forces and advisory groups are established by the steering committee on an ad hoc basis, as necessary to pursue and resolve elements of the program.

The staff of the program comprises AAR employees, personnel contributed on a full- or part-time basis by railroads or members of the supply industry, and personnel under contract to the Federal Railroad Administration or the Transportation Development Agency.

The program plan as presented in 1972 comprised:

1) Phase I -- 1972-1974

Analysis of and interim action regarding the present dynamic aspects of track, equipment, and operations to reduce excessive train action.

2) Phase II -- 1974-1977

Development of improved track and equipment specifications and operating practices to increase dynamic stability.

3) Phase III -- 1977-1982

Application of more advanced scientific principles to railroad track, equipment, and operations to improve dynamic stability.

Phase I officially ended in December of 1974. The major technical elements of Phase I included:

- a) The establishment of the dynamic characteristics of track and equipment.
- b) The development and validation of mathematical models to permit the rapid analysis of the effects on dynamic stability of modifications in design, maintenance, and use of equipment and track structures.
- c) The development of interim guidelines for train handling, makeup, track structures, and engineer training to reduce excessive train action.

The attached report represents the technical manual documentation for the Locomotive Truck Hunting Model, which was developed as an element of item b) above.

ACKNOWLEDGEMENT

The contents of the manual are based largely upon a program developed by Dr. V. K. Garg while working for EMD and Mr. P. W. Hartmann of the Association of American Railroads. Further development and enhancements have been made by Mr. J. G. Tolomei, Consultant, AAR, and by Dr. G. C. Martin, Deputy Project Director of Track-Train Dynamics, and Director-Dynamics Research of the AAR Research and Test Department.

Also, the authors wish to acknowledge Mr. Edward F. Lind, Director, Phase I of the Track-Train Dynamics Research Program. Mr. Lind's leadership has been a major contributing factor to the entire success of the Track-Train Dynamics Research Program--A program which has and will continue to produce significant contributions to the railroad industry for years to come.

Finally, the contributions of man-hours by Electro-Motive Division, General Motors corporation in the model development is deeply appreciated.

This program was developed as part of an effort in Task #7, mathematical modeling of Phase I of the Track-Train Dynamics Research Program.

TABLE OF CONTENTS

	<u>Page</u>
LIST OF ILLUSTRATIONS.....	vi
LIST OF TABLES.....	vii
 <u>SECTION</u>	
I. INTRODUCTION.....	1
II. MATHEMATICAL MODEL AND METHOD OF SOLUTION...	5
III. DISCUSSION OF RESULTS.....	22
IV. CONCLUSIONS.....	28
 <u>APPENDIX</u>	
A. GRAVITATIONAL STIFFNESSES.....	31
B. CREEP.....	35
C. EQUATION OF MOTION FOR 4-AXLE LOCOMOTIVE.....	37
D. EQUATION OF MOTION FOR 6 AXLE LOCOMOTIVE,...	41
E. NOMENCLATURE,.....	50
 BIBLIOGRAPHY.....	 53

LIST OF TABLES

<u>Table</u>		<u>Page</u>
1	Input Data for Act 1 Vehicle	56
2	Input Data for LF1 Locomotive	59
3	Input Data for LS1 Locomotive	62
4	Input Data for LS2, 6-Axle Locomotive	65
5	Summary of Parametric Study of LS2 Locomotive	68
6	Summary of Parametric Study of LF1 Locomotive	69

LIST OF ILLUSTRATIONS

<u>Figure</u>		<u>Page</u>
1	Vehicle Model 6-Axle Locomotive	72
2	Displaced Wheel Set	73
3	Damping Ratio of 4-Axle Vehicle (Act 1) Oscillations	74
4	Characteristic Frequencies of Act 1 Vehicle	75
5	Damping Ratio of 4-Axle Locomotive (LF1) Oscillations	76
6	Characteristic Frequency of LF1 Locomotive	77
7	Critical Speed versus Effective Conicity for LF1	78
8	Damping Ratio of 6-Axle Locomotive (LS1) Oscillations	79
9	Characteristic Frequencies of 6-Axle LS1 Locomotive	80
10	Damping Ratio of 6-Axle Locomotive (LS2) Oscillations	81
11	Characteristic Frequencies of LS2 Locomotive	82
12	Critical Speed versus Lateral Stiffness of Axle for LS2 Locomotive	83
13	Critical Speed versus Effective Wheel Taper for LS2 Locomotive	84
14	Critical Speed versus Lateral Damping for LS2 Locomotive	85
15	Critical Speed versus Carbody Mass and Moment of Inertias for LS2 Locomotive	86
16	Critical Speed versus Truck Fram Mass and Moment of Inertias for LS2 Locomotive	87
17	Critical Speed versus Creep Coefficient for LS2 Locomotive	88
18	Critical Speed versus Truck Wheel Base for LS2 Locomotive	89
B-1	Vehicle Model 4-Axle Locomotive	90
B-2	Creep	91

I. INTRODUCTION

The tendency of a locomotive to oscillate in a lateral plane is commonly referred to as hunting. Hunting results in sustained motions of the locomotive components in which the wheel axle assembly oscillates from rail to rail, the axles and truck yaw about a vertical axis as well as move from side to side, or the carbody responds in the yaw and roll modes. This hunting behavior would occur even if the rails were perfectly aligned and perfectly level.

Hunting oscillations impose severe limitations on achieving a satisfactory ride at high speeds. In addition to reduced ride comfort, the dynamic wheel-rail forces from hunting oscillations can contribute to derailments and rapid wear of locomotive components and track structure.

The hunting oscillation arises from the loss of dynamic stability of the locomotive, which is caused by the speed of the vehicle, the conicity of the wheels, the forces acting between the wheels and the rails, and the reaction of the suspension elements. Hunting is an inherent characteristic and will inevitably occur with all conventional railway vehicles. However, the critical speed at which this behavior first occurs can be increased beyond normal operating speeds by proper selection of such design parameters as wheel tread profile, suspension characteristics, truck geometry, and locomotive weights.

Two very different modes of hunting behavior are frequently observed; body hunting and truck hunting. Body hunting or primary hunting is often characterized by violent motions of the carbody. Sometimes the term "nosing" is used to describe a body hunting mode dominated by yawing motions of the carbody. Body or primary hunting usually occurs over a limited speed range, with both lower and upper bounds on the locomotive speeds. This usually initiates when the frequency of the truck motion equals one of the natural frequencies of carbody motion. The dominant truck frequency is influenced by the conicity of the wheel, and increases nearly in proportion with locomotive speed. Thus, when this dominant frequency coincides with one of the carbody frequencies, primary hunting may occur. Carbody or primary hunting is similar to resonance behavior. This behavior can be controlled by proper damping of the truck suspension system. If the carbody motion is sufficiently damped, body hunting can be eliminated entirely.

Truck hunting, or secondary hunting, is inherent in the vehicle design. Theoretically, with a perfect cylindrical wheel profile, truck hunting can be eliminated, but cylindrical wheel profile has a number of operating drawbacks. This type of hunting is characterized by severe oscillations of the truck or wheel axle set relative to the carbody. Once truck hunting starts, it continues to worsen as locomotive speed increases.

The phenomenon of hunting has been known for many years. However, in 1922, Carter [4]* found that hunting only occurs above certain critical velocities. Since then, extensive theoretical and experimental work has been done by various investigators [1,5,12,13,14].

A complete analysis of the hunting of a locomotive should take into consideration the carbody, truck, primary and secondary suspensions, and the wheel-rail contact forces. This requires a dynamic system with multi-degrees of freedom. Five mathematical models were developed with the objective of evaluating primary and secondary hunting of a four or six-axle locomotive. A two degree of freedom model was developed for a single wheel-axle set. Seven and nine degree of freedom models were developed for trucks with two or three axles. Combining two of the trucks models with the carbody, seventeen and twenty-one degree of freedom locomotive models were obtained. A characteristic equation, based on linear equations of motion was obtained for each model. This equation is a function of velocity. A computer program was written to compute the complex roots (eigenvalues) and the corresponding normalized mode shapes (eigenvectors) of the characteristic equation. This computer program can determine the critical velocity, which is the velocity that coincides with the advent of instability.

* Number in brackets designate references given in Bibliography.

The resulting computer model would be used primarily as a design tool. Using this computer program the effect of different parameters could be simulated at the design stage. Parameters such as suspension stiffness and damping, moment of inertia and mass of locomotive body and truck frame, creep coefficient, and effective conicity could be evaluated to predict critical speed of the locomotive.

In Section 2 the different models are discussed and the equations of motion for the seventeen degree of freedom model are presented. Section 3 includes the results of the 17 and 21 degree of freedom models, along with a discussion on the various parameters which influence the hunting behavior of locomotives. Finally, in section 4 the limitations of the model and suggestions for future improvement are outlined.

II. ANALYTICAL MODEL AND METHOD OF SOLUTION

The problem of modeling a locomotive for lateral stability falls in two categories:

1. The vehicle model with appropriate degrees of freedom.
2. The wheel-rail interaction.

In this section the vehicle models are discussed first; then the wheel-rail interaction are presented using geometrical (effective conicity and gravitational stiffnesses) and dynamic (creep forces) relationships.

2.1 MATHEMATICAL MODELS

Five mathematical models are used for the hunting evaluation. The different models consist of 2, 7, 9, 17 and 21 degrees of freedom. The models are a wheel-axle set, a two or three axle truck frame assembly, and a four or six axle locomotive. Fig. 1 and B-1 illustrate the degrees of freedom and the suspension elements for locomotive models.

The two degree of freedom model is a single wheel-axle assembly consisting of two wheels rigidly connected to an axle. The two degrees of freedom correspond to lateral and yaw motions. The wheel-axle assembly is considered to be isolated from the truck frame by a primary suspension of linear springs and viscous dampers. These primary suspension components are attached in parallel for the longitudinal, lateral and vertical directions. This simple model's behavior is qualitatively similar to that of a complete truck.

A single truck with two or three wheel-axle assemblies comprises the 7 and 9 degree of freedom models, respectively. The wheel-axle assemblies are attached to the truck frame by means of

the primary suspension discussed previously. The truck frame itself is assigned three degrees of freedom consisting of lateral, yaw and roll motions.

Attaching two of the truck models to a rigid car body forms two system models for the 4 and 6 axle locomotives, having 17 and 21 degrees of freedom.

The car body has three degrees of freedom for the lateral, yaw and roll motions. Each truck frame is attached to the car body through a secondary suspension for lateral, yaw and roll motions. The secondary suspension consists of linear springs and viscous dampers connected in parallel.

2.2 THE WHEEL RAIL INTERACTION

2.2.1 GEOMETRICAL RELATIONSHIPS

Traditionally, locomotive wheels are designed with conical wheel treads in order to provide for centering. It has been established [10] that initially, wheel treads wear rapidly and ultimately develop a worn profile which does not undergo further significant change with respect to time [9]. The worn profile does not appear to depend significantly on the original profile of the tread, or on the type of vehicle. Rail heads are similarly worn to a profile, largely independent of the original profile. For small displacements, wheel and rail profiles can be represented by two circular contacting surfaces as shown in Figure 2. This fully defines the system and its effects can be approximated by three linear global

parameters: (1) Effective conicity: It is defined as the change in rolling radius per unit of lateral displacement; (2) Lateral Gravitational Stiffness: It is defined as the rate of change of the net lateral force on the wheel set per unit of lateral displacement; (3) Yaw Gravitational Stiffness: It is defined as the rate of change of the net torque on the wheel set per unit of yaw displacement.

Appendix A contains derivations of lateral and yaw gravitational stiffnesses.

2.2.2 CREEP FORCES

As a wheel set moves along the rails and undergoes yaw and lateral motions, both the wheels and the rails will deform elastically at the contact regions. Creep forces and moments arise due to the difference in strain rates of wheel and rail in the contact region. Creep forces and moment play an important role in lateral instability. Carter [5] was first to recognize their importance and to predict quantitatively the existence of critical speeds.

Linear creep theory assumes that creep forces and moments are directly proportional to the product of $\frac{1}{\text{Forward Speed}}$ and the relative linear and angular velocities of the wheel and rail at the point of contact. For small creepages, Kalker [8] has shown the creep forces are proportional to amount of creep. These constants of proportionality are called "creep coefficients." In the analysis the effect of spin creep is included along with lateral and longitudinal creep forces. Appendix B contains derivations of the creep relationships.

2.3 EQUATION OF MOTION

Equations of motion are developed for two mathematical models; a 17 degree freedom model for a four-axle locomotive, and a 21 degree freedom model for a six-axle locomotive. In the following section a condensed derivation of the equations of motion for the four-axle locomotive is given. Detailed equations of motion for the four and six-axle locomotives have been included in Appendices C and D.

The following assumptions are made in the analysis:

1. The truck frame and carbody are each regarded as perfectly rigid and their stiffness is lumped in the suspension elements.
2. The axles are assumed to run freely in the journal bearing without bearing friction.
3. Lateral clearance between the wheel sets and truck frame is neglected.
4. All displacements are considered small.
5. All springs are assumed to be linear.
6. The vehicle is considered to be symmetric about a vertical plane. This symmetry results in a set of equations of motion in which the vertical motions (bounce and pitch) are uncoupled from the lateral motions (roll, yaw and lateral displacement) when the equations are linearized. Coupling of the vertical and lateral motions through the non-linear characteristics of certain suspension elements and the wheel-rail interaction forces has been ignored.

Equations for longitudinal motion are also uncoupled due to the assumptions of symmetry and small displacement.

7. Non-linearities arising from suspension stops, the wheel flange contact, dry friction in suspension elements, and the adhesion limits between wheel and rail are neglected.

The model shown in Fig. B-1 is used for the hunting study of the four axle locomotive. This represents a 17-degree-of-freedom model of a locomotive consisting of a carbody and two, 2-axle trucks. The carbody is assumed to be rigid and the assigned degrees of freedom are lateral displacement y^b , yaw angle ψ^b and roll angle ϕ^b . Each truck includes lateral y_i^a and yaw ψ_i^a motions for each wheel-axle set and lateral y_j^t , yaw ψ_j^t and roll ϕ_j^t motions for the truck frame.

The wheel-axle sets are connected to the truck frame and the truck frames are connected to the body by the previously described suspension elements. Each wheel-axle set may have different parameters associated with it; but for the sake of notational simplicity, this is ignored in the following analysis.

Relative displacements between the carbody and the two trucks are represented by the vectors:

$$\{U_1\} = [T_1^t] \{U_1^t\} - [T_1^b] \{U^b\} \quad (1)$$

$$\{U_2\} = [T_2^t] \{U_2^t\} - [T_2^b] \{U^b\} \quad (2)$$

Where $\{U_1\}$ represents the relative displacements in the spring between the carbody and truck 1 (leading) in the y and z directions for the left and right side of the truck. $\{U_2\}$ represents the relative displacements for truck 2 (trailing).

$$\{U_1\} = \begin{bmatrix} U_{1L}^Y & U_{1L}^Z & U_{1R}^Y & U_{1R}^Z \end{bmatrix}^T \quad (3a)$$

$$\{U_2\} = \begin{bmatrix} U_{2L}^Y & U_{2L}^Z & U_{2R}^Y & U_{2R}^Z \end{bmatrix}^T \quad (3b)$$

in which $[]^T$ indicates transposed matrix.

The displacement vectors with respect to fixed axes $\{U^b\}$, $\{U_1^t\}$ and $\{U_2^t\}$ for the carbody, leading and trailing trucks are:

$$\{U^b\} = \begin{bmatrix} Y^b & \phi^b & \psi^b \end{bmatrix}^T \quad (4a)$$

$$\{U_1^t\} = \begin{bmatrix} Y_1^t & \phi_1^t & \psi_1^t \end{bmatrix}^T \quad (4b)$$

$$\{U_2^t\} = \begin{bmatrix} Y_2^t & \phi_2^t & \psi_2^t \end{bmatrix}^T \quad (4c)$$

In Equations (1) and (2), $[T_1^b]$ and $[T_1^t]$ are the transfer matrices for the leading truck; $[T_2^b]$ and $[T_2^t]$ are the transfer matrices for the trailing truck.

$$[T_1^b] = \begin{bmatrix} 1 & h_2 & L \\ 0 & -b_2 & 0 \\ 1 & h_2 & L \\ 0 & b_2 & 0 \end{bmatrix} \quad [T_2^b] = \begin{bmatrix} 1 & h_2 & -L \\ 0 & -b_2 & 0 \\ 1 & h_2 & -L \\ 0 & b_2 & 0 \end{bmatrix} \quad (5a, b)$$

$$[T_1^t] = [T_2^t] = \begin{bmatrix} 1 & -h_1 & 0 \\ 0 & -b_2 & 0 \\ 1 & -h_1 & 0 \\ 0 & b_2 & 0 \end{bmatrix} \quad (5c)$$

similarly, relative displacement vector between the truck frame and kth axle is:

$$\{\bar{U}_k\} = [T^a] \{U_k^a\} - [T_k^a] \{U_1^t\} \quad (6)$$

where $k = 1, 2$ and corresponds to leading truck axles.

$$\{\bar{U}_k\} = [T^a] \{U_k^a\} - [T_k^a] \{U_2^t\} \quad (7)$$

where $k = 3, 4$ and corresponds to trailing truck axles.

The vector $\{\bar{U}_k\}$ representing the relative displacements in the y and z direction springs between the truck and axles on the left and right side of the truck frame is:

$$\{\bar{U}_k\} = [\bar{U}_{kL}^y \quad \bar{U}_{kL}^z \quad \bar{U}_{kR}^y \quad \bar{U}_{kR}^z]^T \quad (8)$$

The displacement vector with respect to fixed axes of the k'th axle is:

$$\{U_k^a\} = [Y_k^a \quad \psi_k^a]^T \quad (9)$$

The transfer matrices are:

$$[T^a] = \begin{bmatrix} 1 & 0 \\ 0 & 0 \\ 1 & 0 \\ 0 & 0 \end{bmatrix}; \quad [T_k^a] = \begin{bmatrix} 1 & h_t & (-1)^{k-1} a_k \\ 0 & b_l & 0 \\ 0 & h_t & (-1)^{k-1} a_k \\ 0 & b_l & 0 \end{bmatrix} \quad (10a,b)$$

$k=1, 2, 3, 4$

The potential energy V of the entire system is:

$$V = \frac{1}{2} \{U_1\}^T [K_s] \{U_1\} + \frac{1}{2} \{U_2\}^T [K_s] \{U_2\} \quad (11)$$

$$+ \frac{1}{2} \sum_{k=1}^4 \{\bar{U}_k\}^T [K_p] \{\bar{U}_k\}$$

where $[K_s]$ and $[k_p]$ are the spring stiffness matrices for the secondary and primary suspension systems and are given as:

$$[K_s] = \begin{bmatrix} k_{yt} & & & \\ & k_{zt} & & \\ & & k_{yt} & \\ & & & k_{zt} \end{bmatrix}, \quad [K_p] = \begin{bmatrix} k_{ya} & & & \\ & k_{za} & & \\ & & k_{ya} & \\ & & & k_{za} \end{bmatrix} \quad (12a,b)$$

in which k_{yt} and k_{zt} are the lateral and vertical stiffness of the spring located between the truck frames and carbody; k_{ya} and k_{za} are the lateral and vertical stiffness of the spring located between the truck frame and wheel-axle set. Similarly, the kinetic energy T of the entire system is:

$$T = \frac{1}{2} \{\dot{U}_b\}^T [M^b] \{\dot{U}_b\} + \frac{1}{2} \{\dot{U}_1^t\}^T [M^t] \{\dot{U}_1^t\} \quad (13)$$

$$+ \frac{1}{2} \{\dot{U}_2^t\}^T [M^t] \{\dot{U}_2^t\} + \frac{1}{2} \sum_{k=1}^4 \{\dot{U}_k^a\}^T [M^a] \{\dot{U}_k^a\}$$

Where $[M^b]$, $[M^t]$, and $[M^a]$ are the mass matrices for the carbody, truck frame and wheel-axle set, respectively.

$$[M^b] = \begin{bmatrix} m_B & & \\ & J_B & \\ & & I_B \end{bmatrix}, \quad [M^t] = \begin{bmatrix} m_t & & \\ & J_t & \\ & & I_t \end{bmatrix}, \quad [M^a] = \begin{bmatrix} m_w & & \\ & & I_w \end{bmatrix} \quad (14a,b,c)$$

where m_B , m_t , and m_w represent mass of the carbody, truck frame and wheel-axle set. J_B and J_t refer to roll moment of inertias of the carbody and truck frame. I_B , I_t , and I_w denote yaw moment of inertias of the carbody, truck frame and wheel-axle set.

Finally, the dissipative energy \tilde{D} of the system is given as:

$$\begin{aligned} \tilde{D} = & \frac{1}{2} \{\dot{U}_1\}^T [C_s] \{\dot{U}_1\} + \frac{1}{2} \{\dot{U}_2\}^T [C_s] \{\dot{U}_2\} \quad (15) \\ & + \frac{1}{2} \sum_{k=1}^4 \{\dot{U}_k\}^T [C_p] \{\dot{U}_k\} \end{aligned}$$

where $[C_s]$ and $[C_p]$ are the damping matrices associated with the secondary and primary systems and are given as:

$$[C_s] = \begin{bmatrix} C_{yt} & & & \\ & C_{zt} & & \\ & & C_{yt} & \\ & & & C_{zt} \end{bmatrix}, \quad [C_p] = \begin{bmatrix} C_{ya} & & & \\ & C_{za} & & \\ & & C_{ya} & \\ & & & C_{za} \end{bmatrix} \quad (16a,b)$$

in which C_{yt} and C_{zt} denote the constants of the lateral and vertical damper units located between the truck frame and carbody; C_{ya} and C_{za} are constants of the lateral and vertical damper units located between the truck frame and wheel-axle set.

Now, using a generalized displacement vector $\{x\} = [{}^d_M]$

$$\{x\} = [\{U^b\} \quad \{U_1^t\} \quad \{U_2^t\} \quad \{U_k^a\}]^T \quad (17)$$

for the system and applying Lagrange's equation for each of the generalized coordinates, the equation of motion for the system can be written as:

$$[M] \{\ddot{x}\} + [C'] \{\dot{x}\} + [K'] \{x\} = \begin{bmatrix} \{0\} \\ \{Q\} \end{bmatrix} \quad (18)$$

where $[M]$, $[C']$ and $[K']$ are 17 x 17 square matrices representing respectively the mass, damping and stiffness of the system; $\{Q\}$ is an eight element vector representing the generalized forces acting between the wheels and rails. The expressions for these forces are similar to those give by Wickens [14].

$$\{Q\} = -[K_g] \{U_k^a\} - [C_g] \{\dot{U}_k^a\} \quad (19)$$

where $[K_g]$ and $[C_g]$ are matrices which include the effect of gravity and creep forces resulting from the difference in strain rates of wheel and rail in the contact region.

$$[K_g] = \begin{bmatrix} k'_g & & & \\ & k'_g & & \\ & & k'_g & \\ & & & k'_g \end{bmatrix}, \quad (20a,b)$$

$$[k'_g] = \begin{bmatrix} k_g & -2f_L \\ 2(f_T \lambda b - f_{S33} \epsilon / b) / r & -k_{gw} \end{bmatrix}$$

$$C_g = \begin{bmatrix} c'_g & & & & \\ & c'_g & & & \\ & & c'_g & & \\ & & & c'_g & \\ & & & & c'_g \end{bmatrix}, \quad [C'_g] = \begin{bmatrix} 2f_L/v & & & & \\ & 2f_{S23}/v & & & \\ & & 2(f_T b^2 + f_{S33})/v & & \\ & & & 2f_{S23}/v & \\ & & & & 2f_L/v \end{bmatrix} \quad (20c,d)$$

in which f_T and f_L are creep coefficients in the longitudinal (tangential) and lateral directions and f_{S23} and f_{S33} are spin creep coefficients; k_g and k_{gw} are the lateral and yaw gravitational stiffnesses which mainly depend upon the shape of wheel tread and rail head profiles; λ is the effective conicity; r is the wheel radius; ϵ is a wheel-rail contact parameter; v is the speed of the vehicle.

Substituting Equation (19) into Equation (18), we can rewrite Equation (18) as:

$$[M] \{\ddot{X}\} + [C] \{\dot{X}\} + [K] \{X\} = \{0\} \quad (21)$$

where $\{0\}$ is a 17 element vector, with all elements equal to zero.

2.4 THE EIGENPROBLEM

It is possible to convert the equation of motion from a second degree differential equation in n unknowns to a first degree differential equation with $2n$ unknowns. Pre-multiplying the equation of motion by $[K]^{-1}$ gives:

$$[K]^{-1} [M] \{\ddot{X}\} + [K]^{-1} [C] \{\dot{X}\} + [K]^{-1} [K] \{X\} = [K]^{-1} \{0\}$$

and (22)

$$[K]^{-1} [M] \{\ddot{X}\} + [K]^{-1} [C] \{\dot{X}\} + \{X\} = \{0\} \quad (23)$$

solving for $\{X\}$ in Equation (23) results in

$$\{X\} = -[K]^{-1} [M] \{\ddot{X}\} - [K]^{-1} [C] \{\dot{X}\} \quad (24)$$

Let

$$\{Z\} = \begin{Bmatrix} \{\dot{X}\} \\ \{X\} \end{Bmatrix} \quad (25)$$

be the new unknown vector with 2n elements; from a simple identity and Equation (24)

$$\begin{Bmatrix} \{\dot{X}\} \\ \{X\} \end{Bmatrix} = \begin{bmatrix} \{\dot{X}\} \\ -[K]^{-1} [M] \{\dot{X}\} - [K]^{-1} [C] \{\dot{X}\} \end{bmatrix} \quad (26)$$

factoring out the unknowns from the right hand matrix:

$$\begin{Bmatrix} \{\dot{X}\} \\ \{X\} \end{Bmatrix} = \begin{bmatrix} [O] & [I] \\ -[K]^{-1} [M] & -[K]^{-1} [C] \end{bmatrix} \begin{Bmatrix} \{\ddot{X}\} \\ \{\dot{X}\} \end{Bmatrix} \quad (27)$$

Let

$$[A] = \begin{bmatrix} [O] & [I] \\ -[K]^{-1} [M] & -[K]^{-1} [C] \end{bmatrix} \quad (28)$$

be a 2n x 2n matrix. Then substituting [A] into Equation (27)

$$\begin{Bmatrix} \{\dot{X}\} \\ \{X\} \end{Bmatrix} = [A] \begin{Bmatrix} \{\ddot{X}\} \\ \{\dot{X}\} \end{Bmatrix} \quad (29)$$

Now substitute {Z} of Equation (25) into Equation (29).

$$\{Z\} = [A] \{\dot{Z}\} \quad (30)$$

which is the matrix form of 2n first degree differential equations with 2n unknowns.

Assume a solution $\{Z\} = \{W_k\} e^{\lambda_k t}$ (31)

where $\{W_k\}$ is a 2nx1 constant column matrix. Substitute this into Equation (30).

$$\{W_k\} e^{\lambda_k t} = [A] \{W_k\} \lambda_k e^{\lambda_k t} \quad (32)$$

Divide both sides of Equation (32) by $\lambda_k e^{\lambda_k t}$

$$\{W_k\} \frac{1}{\lambda_k} = [A] \{W_k\} \quad (33)$$

Which is one way of expressing the standard eigenproblem.

An alternative way of developing such an equation is to start by premultiplying the equation of motion (21) by $[M]^{-1}$

$$[M]^{-1} [M] \{\ddot{X}\} + [M]^{-1} [C] \{\dot{X}\} + [M]^{-1} [K] \{X\} = [M]^{-1} \{0\} \quad (34)$$

$$\{\ddot{X}\} + [M]^{-1} [C] \{\dot{X}\} + [M]^{-1} [K] \{X\} = \{0\} \quad (35)$$

solving for $\{\ddot{X}\}$ in Equation (35) results in

$$\{\ddot{X}\} = -[M]^{-1} [C] \{\dot{X}\} - [M]^{-1} [K] \{X\} \quad (36)$$

adding a simple identity to Equation (36) results in the matrix equation

$$\begin{Bmatrix} \{\ddot{X}\} \\ \{\dot{X}\} \end{Bmatrix} = \begin{Bmatrix} -[M]^{-1} [C] \{\dot{X}\} & -[M]^{-1} [K] \{X\} \\ & \{\dot{X}\} \end{Bmatrix} \quad (37)$$

Factor the right hand matrix

$$\begin{Bmatrix} \{\ddot{X}\} \\ \{\dot{X}\} \end{Bmatrix} = \begin{bmatrix} -[M]^{-1} [C] & -[M]^{-1} [K] \\ [I] & [O] \end{bmatrix} \begin{Bmatrix} \{\dot{X}\} \\ \{X\} \end{Bmatrix} \quad (38)$$

It is quite easy to verify that

$$[A]^{-1} = \begin{bmatrix} -[M]^{-1} [C] & -[M]^{-1} [K] \\ [I] & [O] \end{bmatrix} \quad (39)$$

Substitute Equation (39) into Equation (38)

$$\begin{Bmatrix} \{\ddot{X}\} \\ \{\dot{X}\} \end{Bmatrix} = [A]^{-1} \begin{Bmatrix} \{\dot{X}\} \\ \{X\} \end{Bmatrix} \quad (40)$$

Substitute Equation (25) into Equation (40)

$$\{\dot{Z}\} = [A]^{-1} \{Z\} \quad (41)$$

Assume the same solution Equation (31), and substitute it in Equation (41)

$$\{W_k\} \lambda_k e^{\lambda_k t} = [A]^{-1} \{W_k\} e^{\lambda_k t} \quad (42)$$

Divide both sides of Equation (42) by $e^{\lambda_k t}$

$$\{W_k\} \lambda_k = [A]^{-1} \{W_k\} \quad (43)$$

Which is another way to state the eigenproblem. Comparing the two ways of stating the eigenproblem.

$$\{W_k\} \frac{1}{\lambda_k} = [A] \{W_k\} \quad (33)$$

or

$$\{W_k\} \lambda_k = [A]^{-1} \{W_k\} \quad (43)$$

The results should be identical. Either $[A]$ or $[A]^{-1}$ is called the Dynamic Matrix.

However, because of the numerical methods used in solving the eigenproblem, the Dynamic Matrix utilizing the inverse of the stiffness matrix produces more accurate results, as it computes the eigenvalues in an ascending order.

Solving the eigenproblem results in finding $2n$ different eigenvalues and their associated eigenvectors. The complete solution of Equations (30) or (41) would be:

$$\{Z(t)\} = \sum_{k=1}^{2n} g_k \{W_k\} e^{\lambda_k t} \quad (44)$$

where $\{W_k\}$ are the eigenvectors

λ_k are the eigenvalues

g_k are constants that are not found by the program since they involve boundary conditions.

Partitioning Equation (44) results in

$$\{Z(t)\} = \begin{Bmatrix} \{\dot{X}(t)\} \\ \{X(t)\} \end{Bmatrix} = \sum_{k=1}^{2n} g_k \begin{Bmatrix} \{Q_k\} \\ \{V_k\} \end{Bmatrix} e^{\lambda_k t} \quad (45)$$

where it was set that

$$\{W_k\} = \begin{Bmatrix} \{Q_k\} \\ \{V_k\} \end{Bmatrix} \quad (46)$$

The solution of the equation of motion would be the bottom half of Equation (45).

$$\{X(t)\} = \sum_{k=1}^{2n} g_k \{V_k\} e^{\lambda_k t} \quad (47)$$

where $\{V_k\}$ is just the bottom half of the eigenvector $\{W_k\}$.

The eigenvectors and eigenvalues occur in complex conjugates pairs since all the matrices in the equation of motion are real.

Let λ_1 and λ_2 , $\{V_1\}$ and $\{V_2\}$ be complex conjugates. Add a conjugate pair to solutions from Equation (47)

$$\{U\} = g_1 \{V_1\} e^{\lambda_1 t} + g_2 \{V_2\} e^{\lambda_2 t} \quad (48)$$

$$\text{let } g_1 = g_2 = g \quad (49)$$

separate $\{V_1\}$ and $\{V_2\}$ into their magnitude and phase.

$$\{V_1\} = \{V_m\} e^{j\theta_i} \quad (50)$$

$$\{V_2\} = \{V_m\} e^{-j\theta_i} \quad (51)$$

separate λ_1 and λ_2 into their real and imaginary parts

$$\lambda_1 = \alpha + j\beta \quad (52a)$$

$$\lambda_2 = \alpha - j\beta \quad (52b)$$

Substitute Equations (49), (50), (51), and (52) into Equation (48).

$$\{U\} = g \{V_m\} e^{j\theta_i} e^{\alpha t} e^{j\beta t} + g \{V_m\} e^{-j\theta_i} e^{\alpha t} e^{-j\beta t} \quad (53)$$

Factor out that which is common

$$\{U\} = g \{V_m\} e^{\alpha t} (e^{j(\theta_i + \beta t)} + e^{-j(\theta_i + \beta t)}) \quad (54)$$

Utilize Euler's Equation.

$$\{U\} = g \{V_m\} e^{\alpha t} 2 \cos(\beta t + \theta_i) \quad (55)$$

let $g' = 2g$

$$\{U\} = g' \{V_{m_i} \cos(\beta t + \theta_i)\} e^{\alpha t} \quad (56)$$

Substitute this into equation (47). The solution of the equation of motion is:

$$\{X\} = \sum_{k=1,3,\dots}^{2n-1} g'_k \{V_{m_i} \cos(\beta_k t + \theta_i)\} e^{\alpha_k t} \quad (57)$$

On the right hand side of Equation (57), the program calculates all the variables except g'_k .

The stability of the locomotive is determined by examining the sign of α_k . If there exists even one positive α_k the oscillation is unstable. β_k indicates the frequency of oscillation associated with the particular mode characterized by $AMP_{k,i}$ and $\theta_{k,i}$ $i=1$ to n .

Listing the matrix elements.

$$\begin{Bmatrix} X_1(t) \\ X_2(t) \\ \vdots \\ X_i(t) \\ \vdots \\ X_n(t) \end{Bmatrix} = \sum_{k=1,3,\dots}^{2n-1} g'_k \begin{Bmatrix} AMP_{k,1} * \cos(\beta_k t + \theta_{k,1}) \\ AMP_{k,2} * \cos(\beta_k t + \theta_{k,2}) \\ \vdots \\ AMP_{k,i} * \cos(\beta_k t + \theta_{k,i}) \\ \vdots \\ AMP_{k,n} * \cos(\beta_k t + \theta_{k,n}) \end{Bmatrix} e^{\alpha_k t} \quad (58)$$

where

$X_i(t)$ is the displacement of the i 'th degree of freedom

g'_k is a constant that is a function of the boundary conditions and is not calculated by the program

$AMP_{k,i}$ is the magnitude of the k 'th eigenvector associated with the i 'th degree of freedom

$\theta_{k,i}$ is the phase angle of the k 'th eigenvector associated with the i 'th degree of freedom

β_k is the frequency of the k 'th eigenvalue

α_k is the damping exponent of the k 'th eigenvalue

2.5 DETERMINATION OF EIGENVALUES AND EIGENVECTORS

The algorithm used to determine eigenvalues and eigenvectors is given by Grad and Brebner (10). The eigenvalues are computed by the Q-R double step method and the eigenvectors by inverse iteration.

First, the following preliminary modifications are carried out to improve the accuracy of the computed results. (i) The matrix is scaled by a sequence of similarity transformation so that the absolute sums of corresponding rows and columns are roughly equal. (ii) The scaled matrix is normalized so that the value of the Euclidean norm is equal to one.

The main part of the process commences with the reduction of the matrix to an upper-Hessenberg form by means of similarity transformations (Householder's method). Then the Q-R double step iterative process is performed on the Hessenberg matrix until all elements of the subdiagonal that converge to zero are in modulus less than $2^{-t} \|H\|_E$ where t is the number of significant digits in the mantissa of a binary floating-point number. The eigenvalues are then extracted from this reduced form.

Inverse iteration is performed on the upper-Hessenberg matrix until the absolute value of the largest component of the right hand vector is greater than the bound $2^t / (100N)$ where N is the order of the matrix. Normally after this bound is achieved, one more step is performed to obtain the computed eigenvector, but at each step

the residuals are computed, and if the residuals of one particular step are greater in absolute value than the residuals of the previous step, then the vector of the previous step is accepted as the computed eigenvector.

III. DISCUSSION OF RESULTS

In order to verify the results, the program is applied to four vehicle models; two 4-axle locomotives and two 6-axle locomotives. The 4-axle models used in this study are the proposed advanced concept train 1 vehicle (Act 1) and the LF1 locomotive. The input data for these vehicles are given in Tables 1 and 2. The 6-axle models are the LS1 and the LS2 locomotives. Data for these locomotives are shown in Tables 3 and 4. The results of the 4-axle models are discussed first, later the result of the 6-axle models are presented, Finally, parametric studies based on the LS2 and LF1 locomotives are given to evaluate the influence of various parameters on critical speed.

The results for the Act 1 vehicle are shown in Figures 3 and 4. In Figure 4 the carbody and truck frame lateral natural frequencies and the frequency corresponding to the wheel set motion are shown. The damping ratio (decay ratio) versus speed relationship has been plotted in Figure 3. The motion is stable for negative values of the damping ratio, but it is unstable for the positive values. Thus, the critical speed

of hunting is obtained when the value becomes zero. As shown in Figure 3, the instability for the Act 1 vehicle is due to lateral motion of wheel set at the critical speed of 135 mph.

The results of the LF1 locomotive are shown in Figures 5 and 6. The behavior of the locomotive is similar to the Act 1 vehicle. The instability is due to lateral motion of the wheel set at the critical speed of 139.5 mph. In Figure 7 a variation of the critical speed of the LF1 locomotive with respect to the wheel effective conicity is shown. The critical speeds are 139.5 mph for a 1 in 20 taper, and 95.2 mph for a 1 in 10 taper. As the wheel becomes worn, the effective conicity is increased. Experimentally it has been observed [13] that a new 1 in 20 wheel profile is worn to an effective conicity ranging from 1 in 10 to 1 in 6. This suggests that the LF1 locomotive with a worn wheel profile is likely to hunt between a speed of 78 mph to 95 mph. The importance of using a small taper angle initially to achieve high speed is very apparent.

The results for the LS1 and LS2 locomotives are shown in Figure 8, 9, 10, and 11 for speeds greater than 60 mph. With a new 1 in 20 profile the LS1 and LS2 locomotives are unstable at speeds of 101 mph and 121.5 mph, respectively. In both the locomotives instability is due

to lateral motion of the wheel axle set. This indicates that at high speeds the behavior of the 4-axle and 6-axle locomotives is similar from the stability consideration; they both exhibit hunting of the wheel-axle set.

The influence of various parameters on the critical speed was evaluated by first using the basic data of the LS2 6-axle locomotive with high adhesion trucks. The critical speed was calculated as a function of several parameters. The following parameters were studied:

- (1) Lateral stiffness of the primary suspension (wheel set).
- (2) Primary and secondary lateral damping.
- (3) Mass and moment of inertia of the body.
- (4) Mass and moment of inertia of the truck frame.
- (5) Creep coefficient
- (6) Effective conicity (taper angle).

In all the cases, the instability was due to the lateral oscillations of the wheel-axle sets with the largest lateral oscillations occurring at the leading axle.

It was found that varying the lateral stiffness of the wheel axle set from 60% to 140% of its basic value of 5000 lb./in. resulted in the change of critical speed from 100 mph to 139 mph, Figure 12. A change in the effective wheel taper from 0.15 (1 in 6.67) to 0.025 (1 in 40) resulted in an increase of the critical speed from 66 mph to 180 mph, Figure 13.

The influence of lateral damping was studied by independently varying lateral primary and secondary damping. It was observed that the lateral secondary suspension damping has very little

influence on the critical speed of the vehicle. But a change in the lateral primary damping from 200 lb.-sec./in. to 600 lb.-sec./in. resulted in an increase of critical speed from 113 mph to 128 mph; Figure 14.

The mass and moment of inertia of the carbody did not have a significant effect on critical speed, Figure 15. The critical speed was decreased only by 2% with an increase of 100% in the yaw moment of inertia of the body.

The mass and moment of inertia in roll of the truck frame had no effect on the critical speed of the locomotive. However, the critical speed is reduced from 121 mph to 106 mph, when the moment of inertia of the truck frame in yaw is increased by 50%, Figure 16. The yaw moment of inertia of the wheel axle set has a small influence on the critical speed. An increase of 50% in the yaw moment of inertia of the wheel-axle set decreased the critical speed from 121 mph to 116 mph, Figure 16.

Increasing the lateral creep coefficient from 2×10^6 lb/wheel to 6×10^6 lb/wheel resulted in an increase in the critical speed from 109 mph to 121 mph, Figure 17. On the other hand, the same range of values of the tangential creep coefficient caused a decrease in the critical speed. The critical speed was reduced from 152 mph to 110 mph.

From the result of the parametric study, Table 5, it can be concluded that the following parameters (listed in order of importance) are significant for stability of the locomotive at high speed:

1. Effective wheel taper angle.
2. Lateral stiffness of the primary suspension.
3. Creep coefficient.
4. Yaw moment of inertia of the truck frame.
5. Lateral damping of the primary suspension.
6. Yaw moment of inertia of the wheel set.

For speeds lower than 60 mph, the LS1 locomotive became unstable around 40 mph exhibiting body (primary) hunting; however the LS2 locomotive did not show this behavior until the lateral damping was reduced considerably. With a small value of the lateral damping the LS2 locomotive showed body hunting around 30 mph and all speeds in excess of 30 mph. This behavior is different than the LS1 locomotive which has a limited region of primary hunting. It was also found the longitudinal damping had no significant effect on primary and secondary hunting.

Finally the influence of various parameters on both primary and secondary hunting was investigated by using the LF1 locomotive.

Primary hunting was characterized by lateral motion of the trucks being out of phase which corresponded with yaw motion of the body. Secondary hunting was due to lateral oscillations of the wheel axle sets.

The complete results are give in Table 6 page 69. The results concerning secondary hunting confirmed the preceeding conclusions.

The results concerning primary hunting showed that by changing certain parameters, primary hunting could be eliminated. Those variables and the changes necessary to prevent primary hunting are listed below in decreasing order of significance.

- 1) Increase the Lateral damping of the Truck
- 2) Increase the Lateral damping of the Axle
- 3) Increase the Effective conicity
- 4) Increase the Lateral Creep Coefficient
- 5) Increase the distance between Trucks
- 6) Increase the wheel base
- 7) Decrease the moment of inertia of the Body of Yaw
- 8) Decrease the Tangential Creep Coefficient.

Some of the above actions will decrease the critical speed of secondary hunting; therefore, in order to maximize the critical speed and to eliminate primary hunting, it was necessary to combine several different changes in parameters. For example, by increasing the Lateral damping of the truck and decreasing the effective wheel conicity, primary hunting was eliminated and the critical speed was increased.

IV. CONCLUSIONS

The analysis provides a good understanding of the mechanics of lateral oscillations resulting from the hunting behavior of a locomotive based on a linear model of the vehicle. The analysis should give good results for well maintained locomotives operating on good roadbeds on straight track. However, for locomotives travelling on track with large lateral and vertical irregularities and negotiating sharp curves, the non-linearities which result from flange contact, wheel slip, friction, and mechanical stops should be taken into account. In addition, it is necessary to include the non-linearities arising from the response of wheel flange/rail contact, worn wheel profiles, and the non-linear friction creep relationship. If all these non-linearities are included in the model, the model would be too complex and its utility would suffer due to the difficulties in supplying accurate input data, solving the resulting equations of motion, and interpreting the results. As the model used in this analysis neglects all the non-linearities, a one to one correspondence of the calculated results to the experimental results is difficult, but the analysis does provide results within a reasonable accuracy. The real value of the analysis lies in the study of various parameters at the design stage. It should be noted that the accuracy of the results obtained from the analysis is very much dependent upon the accuracy of the input data. In some situations, it may be difficult to supply accurate input for various items; in such cases

it is suggested that the user should select a reasonable number to use as an initial guess and later analyze the effect of these items on the computed results.

Extensions to the model are needed to fully understand the influence of various non-linearities on locomotive response. Well planned experimental work is required to validate the model. As there are many non-linear characteristics inherent in the design of a locomotive, it is essential that the most important of these characteristics be included in the model based on the experimental results.

Next page is blank in original document

APPENDICES

APPENDIX A

GRAVITATIONAL STIFFNESSES

When a wheel set is displaced laterally a small distance y , Fig. 2, the normal reaction forces between the rails and wheels change their direction. Since these forces are large, a small change in their direction produces a significant lateral force on the wheel set.

In the mean position, both tread circles have the same radius r . When the wheel set is displaced laterally, contact occurs at new points and the new angles made by the contact planes after linearization can be given as [7]:

$$\begin{aligned}\delta_1 &= \delta_0 + \frac{y}{(R-R')} \left[\frac{b + R\delta_0}{b - r\delta_0} \right] = \delta_0 + \varepsilon \frac{y}{b} \\ \delta_2 &= \delta_0 - \frac{y}{(R-R')} \left[\frac{b + R\delta_0}{b - r\delta_0} \right] = \delta_0 - \varepsilon \frac{y}{b}\end{aligned}\tag{A-1}$$

where $\varepsilon = \frac{b}{(R-R')} \left(\frac{b + R\delta_0}{b - r\delta_0} \right)$ and is defined as the rate of change of contact plane slope with respect to the lateral displacement of the wheel set. (See note.)

Similarly, the distances between the wheel set centerline and the contact points can be expressed as:

$$\begin{aligned}b_1 &= b - y \left(\frac{R}{R-R'} \right) \left[\frac{b + R'\delta_0}{b - r\delta_0} \right] = b - \xi y \\ b_2 &= b + y \left(\frac{R}{R-R'} \right) \left[\frac{b + R'\delta_0}{b - r\delta_0} \right] = b + \xi y\end{aligned}\tag{A-2}$$

where $\xi = \frac{R}{(R-R')} \left[\frac{b + R'\delta_0}{b - r\delta_0} \right]$ and is known as the rate of change of distance between wheel set centerline and contact points with respect to a lateral displacement of the wheel set (see note).

The tread radii of the wheel at contact points will be:

$$r_1 = r + y \frac{R\delta_0}{(R-R')} \left[\frac{b + R'\delta_0}{b - r\delta_0} \right] = r + \lambda y \quad (\text{A-3})$$

$$r_2 = r - y \frac{R\delta_0}{(R-R')} \left[\frac{b + R'\delta_0}{b - r\delta_0} \right] = r - \lambda y$$

where $\lambda = \frac{R\delta_0}{(R-R')} \left[\frac{b + R'\delta_0}{b - r\delta_0} \right]$; it is often known as

and "effective conicity" which is defined as the rate of change of rolling radius with respect to lateral displacement of the wheel set.

Along with lateral traslation, the wheel set also rotates through an angle ψ . This results in raising the axle load W against gravity through a vertical distance Z which can be written as:

$$Z = \frac{y^2}{2(R-R')} \left[\frac{b + R\delta_0}{b - r\delta_0} \right]^2 - \delta_0 \frac{\psi^2}{2} [b - (R + 2r)\delta_0] \quad (\text{A-4})$$

The work done by the resulting lateral force F_{yg} and couple M_g is equal to the change in potential energy of the system

$$\Delta V = \frac{Wy^2}{2(R-R')} \left[\frac{b + R\delta_0}{b - r\delta_0} \right]^2 - W\delta_0 \frac{\psi^2}{2} [b - (R + 2r)\delta_0] \quad (\text{A-5})$$

Now F_{yg} and M_g can be obtained from (A-5)

$$F_{yg} = \frac{\partial(\Delta V)}{\partial y} = \frac{Wy}{(R-R')} \left[\frac{b + R\delta_0}{b - r\delta_0} \right]^2 \quad (\text{A-6})$$

$$M_g = \frac{\partial(\Delta V)}{\partial \psi} = - W\delta_0 \psi [b - (R + 2r)\delta_0] \quad (\text{A-7})$$

The corresponding lateral and yaw gravitational stiffnesses will be:

$$k_g = \frac{F_{yg}}{y} = \frac{W}{(R-R')} \left[\frac{b + R\delta_0}{b - r\delta_0} \right]^2 \quad (\text{A-8})$$

$$C_g = \frac{M_g}{\psi} = - W\delta_0 [b - (R + 2r)\delta_0] \quad (\text{A-9})$$

When the terms $\frac{\delta_0 r}{b}$ and $(R + 2r)\delta_0^2$ are neglected, (A-8) and (A-9) are reduced to:

$$k_g = \frac{W}{b} (\xi\delta_0 + \epsilon) \quad (\text{A-10})$$

$$C_g = - Wb\delta_0 \quad (\text{A-11})$$

(A-10) and (A-11) are same as given by Wickens [14].

For a perfectly tapered wheel $R \rightarrow \infty$ and by neglecting $\frac{\delta_0 r}{b}$, one obtains:

$$\xi = 1, \quad \epsilon = \delta_0, \quad \text{and} \quad \lambda = \delta_0 \quad (\text{A-12})$$

Thus (A-10) and (A-11) will be reduced to:

$$k_g = \frac{2W\lambda}{b} \quad (\text{A-13})$$

$$C_g = -Wb\lambda \quad (\text{A-14})$$

NOTE: There are alternative expressions for ϵ and ξ given by Blader [2].

$$\epsilon = \frac{b}{R-R'}$$

$$\xi = \frac{2(R+r)}{R-R'}$$

APPENDIX B
CREEP FORCES

Creep forces occur at the wheel tread, when wheel sets undergo lateral, yaw and longitudinal motions. This is a result of the slip that takes place between the wheel and rail at the point of contact. The slip velocity may be analysed by considering separately longitudinal, lateral and spin creep components. (See figure B-2).

Define [4,14] longitudinal creep as

$$CT = \frac{\text{actual forward displacement} - \text{pure rolling lateral displacement}}{\text{forward displacement attributable to rolling}}$$

and define lateral creep as

$$CL = \frac{\text{actual lateral displacement} - \text{pure rolling lateral displacement}}{\text{forward displacement attributable to rolling}}$$

and define spin as

$$SPIN = \frac{\text{actual rotation} - \text{pure rolling rotation}}{\text{forward displacement attributable to rolling}}$$

now

$$CT = \frac{V_t}{V} = \bar{\tau} \left(\frac{\alpha}{r_o} (\text{lateral disp.}) + \frac{b}{v} (\text{yaw vel.}) \right)$$

$$CL = \frac{V_n}{V} = \frac{(\text{lateral vel.})}{v} - (\text{yaw disp.})$$

$$SPIN = \frac{w_n}{V} = \bar{\tau} \frac{\delta}{r_o} + \frac{\text{yaw vel.}}{v}$$

The corresponding creep forces and moments will be:

$$T_t = CT * FT$$

$$T_n = CL * FL + FS23*SPIN$$

$$M = FS23*CL + FS33*SPIN$$

where

FT: tangential or longitudinal creep coefficient
(tangential friction force divided by percent of slip)

FL: lateral creep coefficient (lateral friction force divided by percent of slip)

FS23: Spin creep coefficient

FS33: Spin creep coefficient

The net force exerted by the rail friction on each wheelset is

$$F_t = T_t^{(a)} + T_t^{(b)}$$

$$F_n = T_n^{(a)} + T_n^{(b)}$$

$$M_w = M^{(a)} + M^{(b)} - (T_t^{(a)} - T_t^{(b)})l$$

APPENDIX C

EQUATION OF MOTION FOR 4 - AXLE LOCOMOTIVE

$$\begin{aligned}
 m_w \ddot{y}_1 + k_{yw}(y_1 - y_{t1} - \alpha\psi_{t1} - h_t \dot{\phi}_{t1}) + C_{yw}(\dot{y}_1 - \dot{y}_{t1} - \alpha\dot{\psi}_{t1} - h_t \dot{\phi}_{t1}) \\
 + k_g y_1 + 2f_L \frac{\dot{y}_1}{V} - 2f_L \psi_1 + \frac{2f_{S23}}{V} \dot{\psi}_1 = 0
 \end{aligned} \tag{C-1}$$

$$\begin{aligned}
 m_w \ddot{y}_2 + k_{yw}(y_2 - y_{t1} + \alpha\psi_{t1} - h_t \dot{\phi}_{t1}) + C_{yw}(\dot{y}_2 - \dot{y}_{t1} + \alpha\dot{\psi}_{t1} + h_t \dot{\phi}_{t1}) \\
 + k_g y_2 + 2f_L \frac{\dot{y}_2}{V} - 2f_L \psi_2 + \frac{2f_{S23}}{V} \dot{\psi}_2 = 0
 \end{aligned} \tag{C-2}$$

$$\begin{aligned}
 I_w \ddot{\psi}_1 + k_{\psi w}(\psi_1 - \psi_{t1}) + C_{\psi w}(\dot{\psi}_1 - \dot{\psi}_{t1}) + 2f_T \left(\frac{\lambda b}{r} y_1 + \frac{b^2}{V} \dot{\psi}_1 \right) \\
 - C_g \psi_1 - \frac{2f_{S23}}{V} \dot{y}_1 + \frac{2f_{S33}}{V} \dot{\psi}_1 - \frac{2f_{S33}}{b} \frac{\epsilon}{r} y_1 = 0
 \end{aligned} \tag{C-3}$$

$$\begin{aligned}
 I_w \ddot{\psi}_2 + k_{\psi w}(\psi_2 - \psi_{t1}) + C_{\psi w}(\dot{\psi}_2 - \dot{\psi}_{t1}) + 2f_T \left(\frac{\lambda b}{r} y_2 + \frac{b^2}{V} \dot{\psi}_2 \right) \\
 - C_g \psi_2 - \frac{2f_{S23}}{V} \dot{y}_2 + \frac{2f_{S33}}{V} \dot{\psi}_2 - \frac{2f_{S33}}{b} \frac{\epsilon}{r} y_2 = 0
 \end{aligned} \tag{C-4}$$

$$\begin{aligned}
 m_t \ddot{y}_{T1} - k_{yw}(y_1 - y_{t1} - \alpha\psi_{t1} - h_t \dot{\phi}_{t1}) - C_{yw}(\dot{y}_1 - \dot{y}_{t1} - \alpha\dot{\psi}_{t1} - h_t \dot{\phi}_{t1}) \\
 - k_{yw}(y_2 - y_{t1} + \alpha\psi_{t1} - h_t \dot{\phi}_{t1}) - C_{yw}(\dot{y}_2 - \dot{y}_{t1} + \alpha\dot{\psi}_{t1} - h_t \dot{\phi}_{t1}) \\
 + k_{yt}(y_{t1} - h_1 \phi_{T1} - L\psi_B - h_2 \phi_B - y_B) + C_{yT}(\dot{y}_{t1} - h_1 \dot{\phi}_{t1} - L\dot{\psi}_B \\
 - h_2 \dot{\phi}_B - \dot{y}_B) = 0
 \end{aligned} \tag{C-5}$$

$$\begin{aligned}
 I_t \ddot{\psi}_{t1} - k_{\psi w}(\psi_1 - \psi_{t1}) - C_{\psi w}(\dot{\psi}_1 - \dot{\psi}_{t1}) - k_{\psi w}(\psi_2 - \psi_{t1}) - C_{\psi w}(\dot{\psi}_2 - \dot{\psi}_{t1}) \\
 + k_{\psi t}(\psi_{t1} - \psi_B) + C_{\psi t}(\dot{\psi}_{t1} - \dot{\psi}_B) - k_{yw}\alpha(y_1 - y_{t1} - \alpha\psi_{t1} - h_T \dot{\phi}_{t1}) \\
 - C_{yw}\alpha(\dot{y}_1 - \dot{y}_{t1} - \alpha\dot{\psi}_{t1} - h_t \dot{\phi}_{t1}) + k_{yw}\alpha(y_2 - y_{t1} + \alpha\psi_{t1} - h_t \dot{\phi}_{t1})
 \end{aligned}$$

$$+ c_{yw}(\dot{y}_2 - \dot{y}_{t1} + a\dot{\psi}_{t1} - h_t\dot{\phi}_{t1}) = 0 \quad (\text{C-6})$$

$$\begin{aligned} J_t\ddot{\phi}_{t1} + k_{\theta w}\phi_{t1} + k_{\theta t}(\phi_{t1} - \phi_B) + c_{\theta w}\dot{\phi}_{t1} + c_{\theta t}(\dot{\phi}_{t1} - \dot{\phi}_B) \\ - k_{yt}h_1(y_{t1} - h_1\phi_{t1} - L\psi_B - h_2\phi_B - y_B) - c_{yt}h_1(\dot{y}_{t1} - h_1\dot{\phi}_{t1} - \\ L\dot{\psi}_B - h_2\dot{\phi}_B - \dot{y}_B) \\ - h_t k_{yw}(y_1 - y_{t1} - a\psi_{t1} - h_t\phi_{t1}) - h_t k_{yw}(y_2 - y_{t1} + a\psi_{t1} - h_t\phi_{t1}) \\ - h_t c_{yw}(\dot{y}_1 - \dot{y}_{t1} - a\dot{\psi}_{t1} - h_t\dot{\phi}_{t1}) - h_t c_{yw}(\dot{y}_2 - \dot{y}_{t1} + a\dot{\psi}_{t1} - h_t\dot{\phi}_{t1}) \\ = 0 \end{aligned} \quad (\text{C-7})$$

$$\begin{aligned} M_B\ddot{y}_B - k_{yt}(y_{t1} - h_1\phi_{t1} - L\psi_B - h_2\phi_B - y_B) - c_{yt}(\dot{y}_{t1} - h_1\dot{\phi}_{t1} - L\dot{\psi}_B - \\ h_2\dot{\phi}_B - \dot{y}_B) \\ - k_{yt}(y_{t2} - h_1\phi_{t2} + L\psi_B - h_2\phi_B - y_B) - c_{yt}(\dot{y}_{t2} - h_1\dot{\phi}_{t2} + L\dot{\psi}_B - \\ h_2\dot{\phi}_B - \dot{y}_B) = 0 \end{aligned} \quad (\text{C-8})$$

$$\begin{aligned} I_B\ddot{\psi}_B - k_{yT}L(y_{t1} - h_1\phi_{t1} - L\psi_B - h_2\phi_B - y_B) - c_{yT}L(\dot{y}_{t1} - h_1\dot{\phi}_{t1} - L\dot{\psi}_B - \\ h_2\dot{\phi}_B - \dot{y}_B) \\ + k_{yt}L(y_{t2} - h_2\phi_{t2} + L\psi_B - h_2\phi_B - y_B) + c_{yt}L(\dot{y}_{t2} - h_1\dot{\phi}_{t2} + L\dot{\psi}_B - \\ h_2\dot{\phi}_B - \dot{y}_B) \\ - k_{\psi t}(\psi_{t1} - \psi_B) - c_{\psi t}(\dot{\psi}_{t1} - \dot{\psi}_B) - k_{\psi t}(\psi_{t2} - \psi_B) - c_{\psi t}(\dot{\psi}_{t2} - \dot{\psi}_B) = 0 \end{aligned} \quad (\text{C-9})$$

$$\begin{aligned}
J_B \ddot{\phi}_B - k_{\theta t}(\phi_{t2} - \phi_B) - C_{\theta t}(\dot{\phi}_{t2} - \dot{\phi}_B) - k_{\theta t}(\phi_{t1} - \phi_B) - C_{\theta t}(\dot{\phi}_{t1} - \dot{\phi}_B) \\
- k_{yt} h_2 (y_{t1} - h_1 \phi_{t1} - L\psi_B - h_2 \phi_B - y_B) - C_{yt} h_2 (\dot{y}_{t1} - h_1 \dot{\phi}_{t1} - \\
L\dot{\psi}_B - h_2 \dot{\phi}_B - \dot{y}_B) \\
- k_{yt} h_2 (y_{t2} - h_1 \phi_{t2} + L\psi_B - h_2 \phi_B - y_B) \\
- C_{yt} h_2 (\dot{y}_{t2} - h_1 \dot{\phi}_{t2} + L\dot{\psi}_B - h_2 \dot{\phi}_B - \dot{y}_B) = 0 \quad (C-10)
\end{aligned}$$

$$\begin{aligned}
m_w \ddot{y}_3 + k_{yw} (y_3 - y_{t2} - a\psi_{t2} - h_t \phi_{t2}) + k_g y_3 + 2f_L \left(\frac{\dot{y}_3}{V} - \psi_3 \right) + \frac{2f_{S23}}{V} \dot{\psi}_3 \\
+ C_{yw} (\dot{y}_3 - \dot{y}_{t2} - a\dot{\psi}_{t2} - h_t \dot{\phi}_{t2}) = 0 \quad (C-11)
\end{aligned}$$

$$\begin{aligned}
m_w \ddot{y}_4 + k_{yw} (y_4 - y_{t2} + a\psi_{t2} - h_t \phi_{t2}) + k_g y_4 + 2f_L \left(\frac{\dot{y}_4}{V} - \psi_4 \right) + \frac{2f_{S23}}{V} \dot{\psi}_4 \\
+ C_{yw} (\dot{y}_4 - \dot{y}_{t2} + a\dot{\psi}_{t2} - h_t \dot{\phi}_{t2}) = 0 \quad (C-12)
\end{aligned}$$

$$\begin{aligned}
I_w \ddot{\psi}_3 + k_{\psi w} (\psi_3 - \psi_{t2}) + C_{\psi w} (\dot{\psi}_3 - \dot{\psi}_{t2}) - C_g \psi_3 + 2f_T \left(\frac{\lambda b}{r} y_3 + \frac{b^2}{V} \dot{\psi}_3 \right) - \frac{2f_{S23}}{V} \dot{y}_3 \\
+ \frac{2f_{S33}}{V} \dot{\psi}_3 - \frac{2f_{S33}}{b r} \epsilon y_3 = 0 \quad (C-13)
\end{aligned}$$

$$\begin{aligned}
I_w \ddot{\psi}_4 + k_{\psi w} (\psi_4 - \psi_{t2}) + C_{\psi w} (\dot{\psi}_4 - \dot{\psi}_{t2}) - C_g \psi_4 + 2f_T \left(\frac{\lambda b}{r} y_4 + \frac{b^2}{V} \dot{\psi}_4 \right) = \\
- \frac{2f_{S23}}{V} \dot{y}_4 + \frac{2f_{S33}}{V} \dot{\psi}_4 - \frac{2f_{S33}}{b r} \epsilon y_4 = 0 \quad (C-14)
\end{aligned}$$

$$\begin{aligned}
m_t \ddot{y}_{t2} - k_{yw} (y_3 - y_{t2} - a\psi_{t2} - h_t \phi_{t2}) - C_{yw} (\dot{y}_3 - \dot{y}_{t2} - a\dot{\psi}_{t2} - h_t \dot{\phi}_{t2}) \\
- k_{yw} (y_4 - y_{t2} + a\psi_{t2} - h_t \phi_{t2}) - C_{yw} (\dot{y}_4 - \dot{y}_{t2} + a\dot{\psi}_{t2} - h_t \dot{\phi}_{t2}) \\
+ k_{yt} (y_{t2} - h_1 \phi_{t2} + L\psi_B - h_2 \phi_B - y_B) \\
+ C_{yt} (\dot{y}_{t2} - h_1 \dot{\phi}_{t2} + L\dot{\psi}_B - h_2 \dot{\phi}_B - \dot{y}_B) = 0 \quad (C-15)
\end{aligned}$$

$$\begin{aligned}
I_t \ddot{\psi}_{t2} &- k_{\psi w}(\psi_3 - \psi_{t2}) - C_{\psi w}(\dot{\psi}_3 - \dot{\psi}_{t2}) - k_{\psi w}(\psi_4 - \psi_{t2}) - C_{\psi w}(\dot{\psi}_4 - \dot{\psi}_{t2}) \\
&+ k_{\psi t}(\psi_{t2} - \psi_B) + C_{\psi t}(\dot{\psi}_{t2} - \dot{\psi}_B) - k_{yw}^\alpha(y_3 - y_{t2} - \alpha\psi_{t2} - h_t\phi_{t2}) \\
&- C_{yw}^\alpha(\dot{y}_3 - \dot{y}_{t2} - \alpha\dot{\psi}_{t2} - h_t\dot{\phi}_{t2}) + k_{yw}^\alpha(y_4 - y_{t2} + \alpha\psi_{t2} - h_t\phi_{t2}) \\
&+ C_{yw}^\alpha(\dot{y}_4 - \dot{y}_{t2} + \alpha\dot{\psi}_{t2} - h_t\dot{\phi}_{t2}) = 0 \tag{C-16}
\end{aligned}$$

$$\begin{aligned}
J_t \ddot{\phi}_{t2} &+ k_{\theta w}\phi_{t2} + k_{\theta t}(\phi_{t2} - \phi_B) - C_{\theta w}\dot{\phi}_{t2} + C_{\theta t}(\dot{\phi}_{t2} - \dot{\phi}_B) \\
&- k_{yt}h_1(y_{t2} - h_1\phi_{t2} + L\psi_B - h_2\phi_B - y_B) \\
&- C_{yt}h_1(\dot{y}_{t2} - h_1\dot{\phi}_{t2} + L\dot{\psi}_B - h_2\dot{\phi}_B - \dot{y}_B) \\
&- h_t k_{yw}(y_3 - y_{t2} - \alpha\psi_{t2} - h_t\phi_{t2}) \\
&- h_t C_{yw}(\dot{y}_3 - \dot{y}_{t2} - \alpha\dot{\psi}_{t2} - h_t\dot{\phi}_{t2}) \\
&- h_t k_{yw}(y_4 - y_{t2} + \alpha\psi_{t2} - h_t\phi_{t2}) \\
&- h_t C_{yw}(\dot{y}_4 - \dot{y}_{t2} + \alpha\dot{\psi}_{t2} - h_t\dot{\phi}_{t2}) = 0 \tag{C-17}
\end{aligned}$$

APPENDIX D
EQUATIONS OF MOTION
FOR 6-AXLE LOCOMOTIVE

Figure 1 shows the arrangement of a six-axle locomotive. Relative lateral, yaw and roll displacements between carbody and two trucks are:

$$u_{t1} = y_{t1} - h_1\phi_{t1} - (y_B + L\psi_B + h_2\phi_B) \quad D(1a)$$

$$u_{t2} = y_{t2} - h_1\phi_{t2} - (y_B - L\psi_B + h_2\phi_B) \quad D(1b)$$

$$\omega_{t1} = \psi_{t1} - \psi_B \quad D(1c)$$

$$\omega_{t2} = \psi_{t2} - \psi_B \quad D(1d)$$

$$\theta_{t1} = \phi_{t1} - \phi_B \quad D(1e)$$

$$\theta_{t2} = \phi_{t2} - \phi_B \quad D(1f)$$

similarly, relative lateral and yaw displacements between trucks and wheel axle sets are given as:

$$u_1 = y_1 - (y_{t1} + a_1\psi_{t1} + h_t\phi_{t1}) \quad D(2a)$$

$$u_2 = y_2 - (y_{t1} + a_2\psi_{t1} + h_t\phi_{t1}) \quad D(2b)$$

$$u_3 = y_3 - (y_{t1} - a_3\psi_{t1} + h_t\phi_{t1}) \quad D(2c)$$

$$u_4 = y_4 - (y_{t2} + a_1\psi_{t2} + h_t\phi_{t2}) \quad D(2d)$$

$$u_5 = y_5 - (y_{t2} + a_2\psi_{t2} + h_t\phi_{t2}) \quad D(2e)$$

$$u_6 = y_6 - (y_{t2} - a_3\psi_{t2} + h_t\phi_{t2}) \quad D(2f)$$

$$\omega_1 = \psi_1 - \psi_{t1} \quad D(2g)$$

$$\omega_2 = \psi_2 - \psi_{t1} \quad D(2h)$$

$$\omega_3 = \psi_3 - \psi_{t1} \quad D(2i)$$

$$\omega_4 = \psi_4 - \psi_{t2} \quad D(2j)$$

$$\omega_5 = \psi_5 - \psi_{t2} \quad D(2k)$$

$$\omega_6 = \psi_6 - \psi_{t2} \quad D(2l)$$

The kinetic energy T of translation and rotation for the system is

$$\begin{aligned}
 T = & \frac{1}{2} \sum_{i=1}^6 m_w \dot{y}_i^2 + \frac{1}{2} \sum_{i=1}^6 I_w \dot{\Psi}_i^2 + \frac{1}{2} \sum_{j=1}^2 m_t \dot{y}_{tj}^2 \\
 & + \frac{1}{2} \sum_{j=1}^2 I_t \dot{\psi}_{tj}^2 + \frac{1}{2} \sum_{j=1}^2 J_t \dot{\phi}_{tj}^2 + \frac{1}{2} M_B \dot{y}_B^2 \\
 & + \frac{1}{2} I_B \dot{\Psi}_B^2 + \frac{1}{2} J_B \dot{\Phi}_B^2
 \end{aligned} \tag{D (3)}$$

Similarly the potential energy V of the entire system is given by

$$\begin{aligned}
 V = & \frac{1}{2} \sum_{i=1}^6 k_{yw} u_i^2 + \frac{1}{2} \sum_{i=1}^6 k_{\psi w} \omega_i^2 + \frac{1}{2} \sum_{j=1}^2 k_{yt} u_{tj}^2 \\
 & + \frac{1}{2} \sum_{j=1}^2 k_{\psi t} \omega_{tj}^2 + \frac{1}{2} \sum_{j=1}^2 k_{\theta t} \theta_{tj}^2 \\
 & + \frac{1}{2} \sum_{j=1}^2 k_{\theta w} \phi_{tj}^2
 \end{aligned} \tag{D (4)}$$

The dissipative energy D of the entire system is

$$\begin{aligned}
 D = & \frac{1}{2} \sum_{i=1}^6 c_{yw} \dot{u}_i^2 + \frac{1}{2} \sum_{i=1}^6 c_{\psi w} \dot{\omega}_i^2 + \frac{1}{2} \sum_{j=1}^2 c_{yt} \dot{u}_{tj}^2 \\
 & + \frac{1}{2} \sum_{j=1}^2 c_{\psi t} \dot{\omega}_{tj}^2 + \frac{1}{2} \sum_{j=1}^2 c_{\theta t} \dot{\theta}_{tj}^2 \\
 & + \frac{1}{2} \sum_{j=1}^2 c_{\theta w} \dot{\phi}_{tj}^2
 \end{aligned} \tag{D (5)}$$

Equations for generalized forces acting between the wheels and rails are identical to those given by Wickens [14]. In the analysis concerning the wheel-rail contact geometry, parameters are shown to be the same for each wheel for the sake of notational convenience.

In the model, f_L , f_T , f_{S23} , f_{S33} , λ , ϵ , δ , ξ , r , W , C_g , K_g , m_w , and I_w can be different for each wheel-axle set. The equations for the forces and moments acting on the axles of the lead truck are as follows:

$$Q_1 = -2f_L \left(\frac{\dot{y}_1}{v} - \psi_1 \right) - k_g y_1 - \frac{2f_{S23}}{v} \dot{\psi}_1 \quad D(6a)$$

$$Q_2 = -2f_L \left(\frac{\dot{y}_2}{v} - \psi_2 \right) - k_g y_2 - \frac{2f_{S23}}{v} \dot{\psi}_2 \quad D(6b)$$

$$Q_3 = -2f_L \left(\frac{\dot{y}_3}{v} - \psi_3 \right) - k_g y_3 - \frac{2f_{S23}}{v} \dot{\psi}_3 \quad D(6c)$$

$$Q_4 = -2f_T \left(\frac{\lambda b}{r} y_1 + \frac{b^2}{v} \dot{\psi}_1 \right) + c_g \psi_1 + \frac{2f_{S33}}{br} \epsilon y_1 - \frac{2f_{S33}}{v} \dot{\psi}_1 \quad D(6d)$$

$$Q_5 = -2f_T \left(\frac{\lambda b}{r} y_2 + \frac{b^2}{v} \dot{\psi}_2 \right) + c_g \psi_2 + \frac{2f_{S33}}{br} \epsilon y_2 - \frac{2f_{S33}}{v} \dot{\psi}_2 \quad D(6e)$$

$$Q_6 = -2f_T \left(\frac{\lambda b}{r} y_3 + \frac{b^2}{v} \dot{\psi}_3 \right) + c_g \psi_3 + \frac{2f_{S33}}{br} \epsilon y_3 - \frac{2f_{S33}}{v} \dot{\psi}_3 \quad D(6f)$$

Similarly the equations for the forces and moments acting on the axles of the trailing truck are

$$Q_{13} = -2f_L \left(\frac{\dot{y}_4}{v} - \psi_4 \right) - k_g y_4 - \frac{2f_{S23}}{v} \dot{\psi}_4 \quad D(7a)$$

$$Q_{14} = -2f_L \left(\frac{\dot{y}_5}{v} - \psi_5 \right) - k_g y_5 - \frac{2f_{S23}}{v} \dot{\psi}_5 \quad D(7b)$$

$$Q_{15} = -2f_L \left(\frac{\dot{y}_6}{v} - \psi_6 \right) - k_g y_6 - \frac{2f_{S23}}{v} \dot{\psi}_6 \quad D(7c)$$

$$Q_{16} = -2f_T \left(\frac{\lambda b}{r} y_4 + \frac{b^2}{v} \dot{\psi}_4 \right) + c_g \psi_4 + \frac{2f_{S33}}{b r} \epsilon y_4 - \frac{2f_{S33}}{v} \dot{\psi}_4 \quad D(7d)$$

$$Q_{17} = -2f_T \left(\frac{\lambda b}{r} y_5 + \frac{b^2}{v} \dot{\psi}_5 \right) + c_g \psi_5 + \frac{2f_{S33}}{b r} \epsilon y_5 - \frac{2f_{S33}}{v} \dot{\psi}_5 \quad D(7e)$$

$$Q_{18} = -2f_T \left(\frac{\lambda b}{r} y_6 + \frac{b^2}{v} \dot{\psi}_6 \right) + c_g \psi_6 + \frac{2f_{S33}}{b r} \epsilon y_6 - \frac{2f_{S33}}{v} \dot{\psi}_6 \quad D(7f)$$

Using generalized coordinates q_i ($y_1, y_2, y_3, \psi_1, \psi_2, \psi_3, y_{t1}, \psi_{t1}, \phi_{t1}, y_B, \psi_B, \phi_B, y_4, y_5, y_6, \psi_4, \psi_5, \psi_6, y_{t2}, \psi_{t2}$ and ϕ_{t2}) and applying Lagrange's equation

$$\frac{d}{dt} \left(\frac{\partial T}{\partial \dot{q}_i} \right) - \frac{\partial T}{\partial q_i} + \frac{\partial V}{\partial q_i} + \frac{\partial D}{\partial \dot{q}_i} = Q_i \quad D(8)$$

on each generalized coordinate the following simultaneous equations of motion are obtained

Lead Truck

$$m_w \ddot{y}_1 + c_{yw} (\dot{y}_1 - \dot{y}_{t1} - a_1 \dot{\psi}_{t1} - h_t \dot{\phi}_{t1}) + k_{yw} (y_1 - y_{t1} - a_1 \psi_{t1} - h_t \phi_{t1}) + 2f_L \left(\frac{\dot{y}_1}{v} - \psi_1 \right) + k_g y_1 + \frac{2f_{S23}}{v} \dot{\psi}_1 = 0 \quad D(9a)$$

$$m_w \ddot{y}_2 + c_{yw} (\dot{y}_2 - \dot{y}_{t1} - a_2 \dot{\psi}_{t1} - h_t \dot{\phi}_{t1}) + k_{yw} (y_2 - y_{t1} - a_2 \psi_{t1} - h_t \phi_{t1}) + 2f_L \left(\frac{\dot{y}_2}{v} - \psi_2 \right) + k_g y_2 + \frac{2f_{S23}}{v} \dot{\psi}_2 = 0 \quad D(9b)$$

$$m_w \ddot{y}_3 + c_{yw} (\dot{y}_3 - \dot{y}_{t1} + a_3 \dot{\psi}_{t1} - h_t \dot{\phi}_{t1}) + k_{yw} (y_3 - y_{t1} + a_3 \psi_{t1} - h_t \phi_{t1}) + 2f_L \left(\frac{\dot{y}_3}{v} - \psi_3 \right) + k_g y_3 + \frac{2f_{S23}}{v} \dot{\psi}_3 = 0 \quad D(9c)$$

$$I_w \ddot{\psi}_1 + c_{\psi w} (\dot{\psi}_1 - \dot{\psi}_{t1}) + k_{\psi w} (\psi_1 - \psi_{t1}) - \frac{2f_{S33}}{b r} \epsilon y_1 + 2f_T \left(\frac{\lambda b}{r} y_1 + \frac{b^2}{v} \dot{\psi}_1 \right) - c_g \psi_1 - \frac{2f_{S23}}{v} \dot{y}_1 + \frac{2f_{S33}}{v} \dot{\psi}_1 = 0 \quad D(9d)$$

$$I_w \ddot{\psi}_2 + c_{\psi w} (\dot{\psi}_2 - \dot{\psi}_{t1}) + k_{\psi w} (\psi_2 - \psi_{t1}) - \frac{2f_{S33} \epsilon}{b r} y_2 + 2f_T \left(\frac{\lambda b}{r} y_2 + \frac{b^2}{v} \dot{\psi}_2 \right) - c_g \psi_2 - \frac{2f_{S23}}{v} \dot{y}_2 + \frac{2f_{S33}}{v} \dot{\psi}_2 = 0 \quad D(9e)$$

$$I_w \ddot{\psi}_3 + c_{\psi w} (\dot{\psi}_3 - \dot{\psi}_{t1}) + k_{\psi w} (\psi_3 - \psi_{t1}) - \frac{2f_{S33} \epsilon}{b r} y_3 + 2f_T \left(\frac{\lambda b}{r} y_3 + \frac{b^2}{v} \dot{\psi}_3 \right) - c_g \psi_3 - \frac{2f_{S23}}{v} \dot{y}_3 + \frac{2f_{S33}}{v} \dot{\psi}_3 = 0 \quad D(9f)$$

$$m_t \ddot{y}_{t1} - c_{yw} (\dot{y}_1 - \dot{y}_{t1} - a_1 \dot{\psi}_{t1} - h_t \dot{\phi}_{t1}) - c_{yw} (\dot{y}_2 - \dot{y}_{t1} - a_2 \dot{\psi}_{t1} - h_t \dot{\phi}_{t1}) - c_{yw} (\dot{y}_3 - \dot{y}_{t1} + a_3 \dot{\psi}_{t1} - h_t \dot{\phi}_{t1}) - k_{yw} (y_1 - y_{t1} - a_1 \psi_{t1} - h_t \phi_{t1}) - k_{yw} (y_2 - y_{t1} - a_2 \psi_{t1} - h_t \phi_{t1}) - k_{yw} (y_3 - y_{t1} + a_3 \psi_{t1} - h_t \phi_{t1}) + k_{yt} (y_{t1} - y_B - h_1 \phi_{t1} - h_2 \phi_B - L \psi_B) + c_{yt} (\dot{y}_{t1} - \dot{y}_B - h_1 \dot{\phi}_{t1} - h_2 \dot{\phi}_B - L \dot{\psi}_B) = 0 \quad D(9g)$$

$$I_t \ddot{\psi}_{t1} - c_{\psi w} (\dot{\psi}_1 - \dot{\psi}_{t1}) - c_{\psi w} (\dot{\psi}_2 - \dot{\psi}_{t1}) - c_{\psi w} (\dot{\psi}_3 - \dot{\psi}_{t1}) - k_{\psi w} (\psi_1 - \psi_{t1}) - k_{\psi w} (\psi_2 - \psi_{t1}) - k_{\psi w} (\psi_3 - \psi_{t1}) + c_{\psi t} (\dot{\psi}_{t1} - \dot{\psi}_B) + k_{\psi t} (\psi_{t1} - \psi_B) - c_{yw} a_1 (\dot{y}_1 - \dot{y}_{t1} - a_1 \dot{\psi}_{t1} - h_t \dot{\phi}_{t1}) - k_{yw} a_1 (y_1 - y_{t1} - a_1 \psi_{t1} - h_t \phi_{t1}) - c_{yw} a_2 (\dot{y}_2 - \dot{y}_{t1} - a_2 \dot{\psi}_{t1} - h_t \dot{\phi}_{t1}) - k_{yw} a_2 (y_2 - y_{t1} - a_2 \psi_{t1} - h_t \phi_{t1}) + c_{yw} a_3 (\dot{y}_3 - \dot{y}_{t1} + a_3 \dot{\psi}_{t1} - h_t \dot{\phi}_{t1}) + k_{yw} a_3 (y_3 - y_{t1} + a_3 \psi_{t1} - h_t \phi_{t1}) = 0 \quad D(9h)$$

$$\begin{aligned}
J_t \ddot{\phi}_{t1} + k_{\theta w} \phi_{t1} + c_{\theta w} \dot{\phi}_{t1} + k_{\theta t} (\phi_{t1} - \phi_B) + c_{\theta t} (\dot{\phi}_{t1} - \dot{\phi}_B) \\
- h_1 k_{yt} (y_{t1} - y_B - h_2 \phi_B - L \psi_B - h_1 \phi_{t1}) \\
- h_1 c_{yt} (\dot{y}_{t1} - \dot{y}_B - h_2 \dot{\phi}_B - L \dot{\psi}_B - h_1 \dot{\phi}_{t1}) \\
- h_t k_{yw} (y_1 - y_{t1} - a_1 \psi_{t1} - h_t \phi_{t1}) \\
- h_t c_{yw} (\dot{y}_1 - \dot{y}_{t1} - a_1 \dot{\psi}_{t1} - h_t \dot{\phi}_{t1}) \\
- h_t k_{yw} (y_2 - y_{t1} - a_2 \psi_{t1} - h_t \phi_{t1}) \\
- h_t c_{yw} (\dot{y}_2 - \dot{y}_{t1} - a_2 \dot{\psi}_{t1} - h_t \dot{\phi}_{t1}) \\
- h_t k_{yw} (y_3 - y_{t1} + a_3 \psi_{t1} - h_t \phi_{t1}) \\
- h_t c_{yw} (\dot{y}_3 - \dot{y}_{t1} + a_3 \dot{\psi}_{t1} - h_t \dot{\phi}_{t1}) = 0
\end{aligned} \tag{9i}$$

Carbody

$$\begin{aligned}
M_B \ddot{y}_B - k_{yt} (y_{t1} - y_B - h_1 \phi_{t1} - h_2 \phi_B - L \psi_B) \\
- c_{yt} (\dot{y}_{t1} - \dot{y}_B - h_1 \dot{\phi}_{t1} - h_2 \dot{\phi}_B - L \dot{\psi}_B) \\
- k_{yt} (y_{t2} - y_B - h_1 \phi_{t1} - h_2 \phi_B + L \psi_B) \\
- c_{yt} (\dot{y}_{t2} - \dot{y}_B - h_1 \dot{\phi}_{t1} - h_2 \dot{\phi}_B + L \dot{\psi}_B) = 0
\end{aligned} \tag{10a}$$

$$\begin{aligned}
I_B \ddot{\psi}_B - k_{\psi t} (\psi_{t1} - \psi_B) - c_{\psi t} (\dot{\psi}_{t1} - \dot{\psi}_B) - k_{\psi t} (\psi_{t2} - \psi_B) \\
- c_{\psi t} (\dot{\psi}_{t2} - \dot{\psi}_B) - k_{yt} L (y_{t1} - y_B - h_2 \phi_B - h_1 \phi_{t1} - L \psi_B) \\
- c_{yt} L (\dot{y}_{t1} - \dot{y}_B - h_2 \dot{\phi}_B - h_1 \dot{\phi}_{t1} - L \dot{\psi}_B) \\
+ k_{yt} L (y_{t2} - y_B - h_2 \phi_B - h_1 \phi_{t2} + L \psi_B) \\
+ c_{yt} L (\dot{y}_{t2} - \dot{y}_B - h_2 \dot{\phi}_B - h_1 \dot{\phi}_{t2} + L \dot{\psi}_B) = 0
\end{aligned} \tag{10b}$$

$$\begin{aligned}
J_B \ddot{\phi}_B - k_{\theta t} (\phi_{t1} - \phi_B) - c_{\theta t} (\dot{\phi}_{t1} - \dot{\phi}_B) - k_{\theta t} (\phi_{t2} - \phi_B) \\
- c_{\theta t} (\dot{\phi}_{t2} - \dot{\phi}_B) - k_{yt} h_2 (y_{t1} - y_B - h_2 \phi_B - h_1 \phi_{t1} - L \psi_B) \\
- c_{yt} h_2 (\dot{y}_{t1} - \dot{y}_B - h_2 \dot{\phi}_B - h_1 \dot{\phi}_{t1} - L \dot{\psi}_B) \\
- k_{yt} h_2 (y_{t2} - y_B - h_2 \phi_B - h_1 \phi_{t1} + L \psi_B) \\
- c_{yt} h_2 (\dot{y}_{t2} - \dot{y}_B - h_2 \dot{\phi}_B - h_1 \dot{\phi}_{t1} + L \dot{\psi}_B) = 0
\end{aligned} \tag{10c}$$

Trailing Truck

$$m_w \ddot{y}_4 + c_{yw} (\dot{y}_4 - \dot{y}_{t2} - \alpha_1 \dot{\psi}_{t2} - h_t \dot{\phi}_{t2}) + k_{yw} (y_4 - y_{t2} - \alpha_1 \psi_{t2} - h_t \phi_{t2}) + 2f_L \left(\frac{\dot{y}_4}{v} - \dot{\psi}_4 \right) + k_g y_4 + \frac{2f_{S23}}{v} \dot{\psi}_4 = 0 \quad D (11a)$$

$$m_w \ddot{y}_5 + c_{yw} (\dot{y}_5 - \dot{y}_{t2} - \alpha_2 \dot{\psi}_{t2} - h_t \dot{\phi}_{t2}) + k_{yw} (y_5 - y_{t2} - \alpha_2 \psi_{t2} - h_t \phi_{t2}) + 2f_L \left(\frac{\dot{y}_5}{v} - \dot{\psi}_5 \right) + k_g y_5 + \frac{2f_{S23}}{v} \dot{\psi}_5 = 0 \quad D (11b)$$

$$m_w \ddot{y}_6 + c_{yw} (\dot{y}_6 - \dot{y}_{t2} + \alpha_3 \dot{\psi}_{t3} - h_t \dot{\phi}_{t2}) + k_{yw} (y_6 - y_{t2} + \alpha_3 \psi_{t3} - h_t \phi_{t2}) + 2f_L \left(\frac{\dot{y}_6}{v} - \dot{\psi}_6 \right) + k_g y_6 + \frac{2f_{S23}}{v} \dot{\psi}_6 = 0 \quad D (11c)$$

$$I_w \ddot{\psi}_4 + k_{\psi w} (\psi_4 - \psi_{t2}) + c_{\psi w} (\dot{\psi}_4 - \dot{\psi}_{t2}) + 2f_T \left(\frac{\lambda b}{r} y_4 + \frac{b^2}{v} \dot{\psi}_4 \right) - c_g \psi_4 - \frac{2f_{S33}}{b r} \epsilon y_4 - \frac{2f_{S23}}{v} \dot{y}_4 + \frac{2f_{S33}}{v} \dot{\psi}_4 = 0 \quad D (11d)$$

$$I_w \ddot{\psi}_5 + k_{\psi w} (\psi_5 - \psi_{t2}) + c_{\psi w} (\dot{\psi}_5 - \dot{\psi}_{t2}) + 2f_T \left(\frac{\lambda b}{r} y_5 + \frac{b^2}{v} \dot{\psi}_5 \right) - c_g \psi_5 - \frac{2f_{S33}}{b r} \epsilon y_5 - \frac{2f_{S23}}{v} \dot{y}_5 + \frac{2f_{S33}}{v} \dot{\psi}_5 = 0 \quad D (11e)$$

$$I_w \ddot{\psi}_6 + k_{\psi w} (\psi_6 - \psi_{t2}) + c_{\psi w} (\dot{\psi}_6 - \dot{\psi}_{t2}) + 2f_T \left(\frac{\lambda b}{r} y_6 + \frac{b^2}{v} \dot{\psi}_6 \right) - c_g \psi_6 - \frac{2f_{S33}}{b r} \epsilon y_6 - \frac{2f_{S23}}{v} \dot{y}_6 + \frac{2f_{S33}}{v} \dot{\psi}_6 = 0 \quad D (11f)$$

$$m_t \ddot{y}_{t2} - k_{yw} (y_4 - y_{t2} - \alpha_1 \psi_{t2} - h_t \phi_{t2}) - c_{yw} (\dot{y}_4 - \dot{y}_{t2} - \alpha_1 \dot{\psi}_{t2} - h_t \dot{\phi}_{t2}) - k_{yw} (y_5 - y_{t2} - \alpha_2 \psi_{t2} - h_t \phi_{t2}) - c_{yw} (\dot{y}_5 - \dot{y}_{t2} - \alpha_2 \dot{\psi}_{t2} - h_t \dot{\phi}_{t2}) - k_{yt} (y_{t2} - y_B - h_1 \phi_{t2} - h_2 \phi_B + L \psi_B)$$

D (117)

$$\begin{aligned}
& - \dot{c}y^w h^t (\dot{y}_6 - \dot{y} t_2 + a_3 \dot{\psi} t_2 - h^t \dot{\phi} t_2) = 0 \\
& - \dot{c}y^w h^t (\dot{y}_6 - \dot{y} t_2 + a_3 \dot{\psi} t_2 - h^t \dot{\phi} t_2) \\
& - \dot{c}y^w h^t (\dot{y}_5 - \dot{y} t_2 - a_2 \dot{\psi} t_2 - h^t \dot{\phi} t_2) \\
& - \dot{c}y^w h^t (\dot{y}_5 - \dot{y} t_2 - a_2 \dot{\psi} t_2 - h^t \dot{\phi} t_2) \\
& - \dot{c}y^w h^t (\dot{y}_4 - \dot{y} t_2 - a_1 \dot{\psi} t_2 - h^t \dot{\phi} t_2) \\
& - \dot{c}y^w h^t (\dot{y}_4 - \dot{y} t_2 - a_1 \dot{\psi} t_2 - h^t \dot{\phi} t_2) \\
& - \dot{c}y^t h^1 (\dot{y}_B - \dot{y} t_2 - h^1 \dot{\psi} t_2 + L \dot{\psi}_B - h^2 \dot{\phi}_B) \\
& - \dot{c}y^t h^1 (\dot{y}_B - \dot{y} t_2 - h^1 \dot{\psi} t_2 + L \dot{\psi}_B - h^2 \dot{\phi}_B) \\
& \dot{I}^t \dot{\phi} t_2 + \dot{c} \theta w \dot{\phi} t_2 + \dot{c} \theta w \dot{\phi} t_2 + \dot{c} \theta w \dot{\phi} t_2 + \dot{c} \theta w \dot{\phi} t_2 + \dot{c} \theta w \dot{\phi} t_2 - \dot{\phi}_B - \dot{\phi} t_2
\end{aligned}$$

D (118)

$$\begin{aligned}
& 0 = \dot{c}y^w a_3 (\dot{y}_6 - \dot{y} t_2 + a_3 \dot{\psi} t_2 - h^t \dot{\phi} t_2) + \dot{c}y^w a_3 (\dot{y}_6 - \dot{y} t_2 + a_3 \dot{\psi} t_2 - h^t \dot{\phi} t_2) \\
& + \dot{c}y^w a_3 (\dot{y}_6 - \dot{y} t_2 + a_3 \dot{\psi} t_2 - h^t \dot{\phi} t_2) + \dot{c}y^w a_3 (\dot{y}_6 - \dot{y} t_2 + a_3 \dot{\psi} t_2 - h^t \dot{\phi} t_2) \\
& + \dot{c}y^w a_2 (\dot{y}_5 - \dot{y} t_2 - a_2 \dot{\psi} t_2 - h^t \dot{\phi} t_2) + \dot{c}y^w a_2 (\dot{y}_5 - \dot{y} t_2 - a_2 \dot{\psi} t_2 - h^t \dot{\phi} t_2) \\
& + \dot{c}y^w a_2 (\dot{y}_5 - \dot{y} t_2 - a_2 \dot{\psi} t_2 - h^t \dot{\phi} t_2) + \dot{c}y^w a_2 (\dot{y}_5 - \dot{y} t_2 - a_2 \dot{\psi} t_2 - h^t \dot{\phi} t_2) \\
& - \dot{c}y^w a_1 (\dot{y}_4 - \dot{y} t_2 - a_1 \dot{\psi} t_2 - h^t \dot{\phi} t_2) - \dot{c}y^w a_1 (\dot{y}_4 - \dot{y} t_2 - a_1 \dot{\psi} t_2 - h^t \dot{\phi} t_2) \\
& - \dot{c}y^w a_1 (\dot{y}_4 - \dot{y} t_2 - a_1 \dot{\psi} t_2 - h^t \dot{\phi} t_2) - \dot{c}y^w a_1 (\dot{y}_4 - \dot{y} t_2 - a_1 \dot{\psi} t_2 - h^t \dot{\phi} t_2) \\
& + \dot{c} \psi t (\dot{\psi} t_2 - \dot{\psi}_B) + \dot{c} \psi t (\dot{\psi} t_2 - \dot{\psi}_B) + \dot{c} \psi t (\dot{\psi} t_2 - \dot{\psi}_B) \\
& - \dot{c} \psi w (\dot{\psi}_5 - \dot{\psi} t_2) - \dot{c} \psi w (\dot{\psi}_5 - \dot{\psi} t_2) - \dot{c} \psi w (\dot{\psi}_5 - \dot{\psi} t_2) \\
& - \dot{c} \psi w (\dot{\psi}_5 - \dot{\psi} t_2) - \dot{c} \psi w (\dot{\psi}_5 - \dot{\psi} t_2) - \dot{c} \psi w (\dot{\psi}_5 - \dot{\psi} t_2)
\end{aligned}$$

D (119)

$$\begin{aligned}
& - \dot{c}y^w (\dot{y}_6 - \dot{y} t_2 + a_3 \dot{\psi} t_2 - h^t \dot{\phi} t_2) = 0 \\
& - \dot{c}y^w (\dot{y}_6 - \dot{y} t_2 + a_3 \dot{\psi} t_2 - h^t \dot{\phi} t_2) \\
& + \dot{c}y^t (\dot{y}_B - \dot{y} t_2 - h^1 \dot{\psi} t_2 - h^2 \dot{\phi}_B + L \dot{\psi}_B)
\end{aligned}$$

APPENDIX D

NOMENCLATURE

m_w		Axle (wheel set) mass
m_t		Truck frame mass
M_B		Carbody mass
I_w		Axle (wheel set) yaw moment of inertia
I_t		Truck frame yaw moment of inertia
I_B		Carbody yaw moment of inertia
J_t		Truck frame roll moment of inertia
J_B		Carbody roll moment of inertia
k_{yw}		Lateral primary stiffness per axle
k_{xw}		Longitudinal primary stiffness per axle
$k_{\psi w} = b_1^2 \cdot k_{xw}$		Yaw primary stiffness per axle
k_g		Lateral gravitational stiffness for wheel axle set
C_g		Yaw gravitational stiffness for wheel axle set
k_{yt}		Lateral secondary stiffness per truck
$k_{\psi t}$		Yaw secondary stiffness per truck
$k_{\theta t} = 2k_b b_2^2$		Roll secondary stiffness per truck
$k_{\theta w} = 2k_j b_1^2$		Roll primary stiffness per truck
k_j		Vertical primary stiffness per truck side
k_b		Vertical secondary stiffness per truck side

C_{yw}	Lateral primary damping per axle
C_{xw}	Longitudinal primary damping per axle
$C_{\psi w} = b_1^2 \cdot C_{xw}$	Yaw primary damping per axle
C_{yt}	Lateral secondary damping per truck
$C_{\psi t}$	Yaw secondary damping per truck
$C_{\theta t} = 2C_b b_2^2$	Roll secondary damping per truck
$C_{\theta w} = 2C_j b_1^2$	Roll primary damping per truck
C_j	Vertical primary damping per truck side
C_b	Vertical secondary damping per truck side
a	Half of truck wheelbase
b	Half distance between contact points of wheel treads and rails in lateral direction.
b_1	Half lateral distance between primary suspension
b_2	Half lateral distance between secondary suspension
h_B	Height of carbody center of gravity above axle center
h_t	Height of truck frame center of gravity above axle center
h_1	Vertical distance, truck frame center of gravity to secondary suspension
h_2	Vertical distance, carbody center of gravity to secondary suspension

L	Half distance between bolster centers
f_L, f_T	Lateral and tangential creep coefficient
f_{S23}, f_{S33}	Spin creep coefficients
r	Wheel tread radius
v	Locomotive speed
W	Axle load
ζ	Wheel-rail contact geometry parameter
δ	Wheel-rail contact geometry parameter
ϵ	Wheel-rail contact geometry
λ	Effective wheel conicity
y_i	Lateral displacement of wheel axle set ($i = 1, 2, 3, 4, 5,$ and 6 refers to #1, #2, #3, #4, #5, and #6 wheel axle sets respectively)
ψ_i	Yaw displacement of wheel axle set
y_t	Lateral displacement of truck frame (suffixes $t1$ and $t2$ refer to front and rear trucks respectively)
ψ_t	Yaw displacement of truck frame
ϕ_t	Roll displacement of truck frame
y_B	Lateral displacement of carbody
ψ_B	Yaw displacement of carbody
ϕ_B	Roll displacement of carbody

BIBLIOGRAPHY

1. Bishop, R. E. D. "Some Observations on Linear Theory of Railway Vehicle Instability," Proceedings, Inst. Mech. Eng., Vol. 180, Pt. 3F, London, 1965-66.
2. Blader, F. B., and Kurtz, E. F., Jr. "Dynamic Stability of Cars in Long Freight Trains," Rail Transportation Division, ASME, presented at the Winter Annual Meeting, Nov. 11-15, 1973, Paper No. 73-WA/RT-2.
3. Carnahan, Luther, Wilkes, Applied Numerical Methods, N.Y.: J. Wiley and Sons, Inc., 1969, pp. 290-291.
4. Carter, F. W., Railway Electric Traction, London: Arnold, 1922, pp. 57-70.
5. Carter, F. W. "On the Stability of Running Locomotives," Proceedings Royal Society, Series A, 1938, pp.585-611.
6. Gard, J., and Brebner, M. A. "Algorithm 343, Eigenvalues and Eigenvectors of a Real General Matrix (F2)," Communications of the ACM, Vol. 11, No. 12, Dec. 1968 pp. 820-826.
7. Joly, R. "Study of the Transverse Stability of a Railway Vehicle Running at High Speed," Rail International, Feb. 1972.
8. Kalker, J. J. "Transmission of a Force and Couple Between Two Elastically Similar Rolling Spheres," Koninkl Ned Akad Wetenschap, Proc. (Series B), 1964, 67, p. 135.
9. King, B. L. "An Assessment of the Contact Conditions Between Worn Tyres and New Rails in Straight Track," DYN/42, Dec. 1966, British Railways Research Dept., Derby, England.
10. King, B. L. "An Evaluation of the Contact Conditions Between a Pair of Worn Wheels and Worn Rails in Straight Track," DYN/37, Sept. 1966, British Railway Research Dept., Derby, England.

11. Marcotte, P.P. "Lateral Dynamic Stability of Railway Bogie Vehicles," Master of Engineering Thesis presented to University of Sheffield, Sheffield, England, May, 1972.
12. Matsudaira, T. "Hunting Problem of High-Speed Railway Vehicle with Special Reference to Bogie Design for the New Tokaido Line," Proceedings Inst. Mech. Eng. Vol. 180, Pt. 3F, London, 1965-66.
13. Matsudaira, T., Matsui, N., Arai, S., and Yokose, K. "Problems of Hunting of Railway Vehicle on Test Stand," Paper No. 68-WA/RR-2 presented at the Winter Annual Meeting of the ASME, New York, N. Y., Dec. 1-5, 1968.
14. Wickens, A. H. "The Dynamics of Railway Vehicles on Straight Tracks: Fundamental Considerations of Lateral Stability," Proc. Inst. Mech. Eng., Vol. 180, Pt. 3F, London, 1965-66.
15. "Survey of Research in Transportation Technology," The Winter Annual Meeting of ASME, Nov. 11-15, 1973.

Next page is blank in original document

TABLES

TABLE 1
INPUT DATA FOR ACT 1 VEHICLE*

DIMENSIONAL DATA:

A	- Half length of wheel base	=	41.0 in.
B	- Half distance between wheel contact points	=	29.5 in.
B1	- Half lateral distance between primary suspension	=	39.0 in.
B2	- Half lateral distance between secondary suspension	=	12.0 in.
HT	- Height of truck frame center of gravity above axle center	=	0.0 in.
H1	- Height of bolster spring center above truck frame center of gravity	=	9.0 in.
HB	- Height of body center of gravity above axle center	=	53.0 in.
XL	- Half distance between truck centers	=	300.0 in.
RO	- Wheel tread radius	=	14.0 in.

MASS AND INERTIA DATA:

XMB	- Carbody mass	=	241 lb.-sec. ² /in.
XMT	- Truck frame mass	=	18.2 lb.-sec. ² /in.
XMW	- Wheel set mass	=	2.8 lb.-sec. ² /in.
XIB	- Carbody yaw moment of inertia	=	10,350,000 lb.-in.-sec. ²
XJB	- Carbody roll moment of inertia	=	594,000 lb.-in.-sec. ²

* - Data obtained from Transportation Systems Center (TSC) which was received from Battelle Memorial, Columbus, Ohio

TABLE 1 (Cont'd.)

MASS AND INERTIA DATA:

XIT	- Truck frame yaw moment of inertia	=	15,300 lb.-in.-sec. ²
XJT	- Truck frame roll moment of inertia	=	6,810 lb.-in.-sec. ²
XIW	- Wheel set yaw moment of inertia	=	2,120 lb.-in.-sec. ²

SPRING RATES AND DAMPING DATA:

XKYW	- Lateral primary stiffness per axle	=	100,000 lb./in.
XKXW	- Longitudinal primary stiffness per axle	=	1,000,000 lb./in.
XKYT	- Lateral secondary stiffness per truck	=	1,190 lb./in.
XKYAT	- Yaw secondary stiffness per truck	=	0.0 lb.-in./rad.
XKJ	- Vertical primary stiffness per truck side	=	1,000,000 lb./in.
XKB	- Vertical secondary stiffness per truck side	=	5,660 lb./in.
CYW	- Lateral damping of axle	=	0.0 lb.-sec./in.
CXW	- Longitudinal damping of axle	=	0.0 lb.-sec./in.
CYT	- Lateral secondary damping per truck	=	77.2 lb.-in./sec.
CYAT	- Yaw secondary damping per truck	=	0.0 lb.-in./sec.
CJ	- Vertical primary damping per truck side	=	0.0 lb.-in./sec.
CB	- Vertical secondary damping per truck side	=	368.06 lb.-in./sec.

TABLE 1 (Cont'd.)

MISCELLANEOUS DATA:

FL	- Lateral creep coefficient per wheel	=	1,540,000.0 lb.
FT	- Longitudinal creep coefficient per wheel	=	1,540,000.0 lb.
ZETA (ξ)		=	1.0
EPSI (ϵ)		=	0.05
RMO (δ)		=	0.05
XLAMD (λ)	- Effective conicity		0.05
W	- Axle load	=	27,840 lb.

TABLE 2

INPUT DATA FOR LF1 LOCOMOTIVE

DIMENSIONAL DATA:

A	- Half length of wheel base	= 54.0 in.
B	- Half distance between wheel contact points	= 29.5 in.
B1	- Half lateral distance between primary suspension	= 39.5 in.
B2	- Half lateral distance between secondary suspension	= 38.0 in.
HT	- Height of truck frame center of gravity above axle center	= 2.0 in.
H1	- Height of bolster spring center above truck frame center of gravity	= 4.5 in.
HB	- Height of body center of gravity above axle center	= 61.0 in.
H2	- Height of body center of gravity above bolster spring center	= 63.5 in.
XL	- Half distance between truck centers	= 204 in.
RO	- Wheel tread radius	= 20.0 in.

MASS AND INERTIA DATA:

XMB	- Carbody mass	= 546 lb.-in.-sec. ²
XMT	- Truck frame mass	= 19.4 lb.-in.-sec. ²
XMW	- Wheel set mass	= 22.1 lb.-in.-sec. ²
XIB	- Carbody yaw moment of inertia	= 19,800,000 lb.-in.-sec. ²

TABLE 2 (Cont'd.)

MASS AND INERTIA DATA:

XJB	- Carbody roll moment of inertia	=	1,170,000 lb.-in.-sec ²
XIT	- Truck frame yaw moment of inertia	=	20,000 lb.-in.-sec ²
XJT	- Truck frame roll moment of inertia	=	8,120 lb.-in.-sec ²
XIW	- Wheel set yaw moment of inertia	=	12,000 lb.-in.-sec ²

SPRING RATES AND DAMPING DATA:

XKYW	- Lateral primary stiffness per axle	=	8,000 lb./in.
XKXW	- Longitudinal primary stiffness per axle	=	1,000,000 lb./in.
XKYT	- Lateral secondary stiffness per truck	=	2,240 lb./in.
XKYAT	- Yaw secondary stiffness per truck	=	0.0 lb./in.
XKJ	- Vertical primary stiffness per truck side	=	16,152 lb./in.
XKB	- Vertical secondary stiffness per truck side	=	11,300 lb./in.
CYW	- Lateral damping of axle	=	0 lb.-sec./in.
CXW	- Longitudinal damping of axle	=	0 lb.-sec./in.
CYT	- Lateral secondary damping per truck	=	10.0 lb.-sec./in.
CYAT	- Yaw secondary damping per truck	=	0 lb.-sec./in.
CJ	- Vertical primary damping per truck side	=	0 lb.-sec./in.
CB	- Vertical secondary damping per truck side	=	450 lb.-sec./in.

TABLE 2 (Cont'd.)

MISCELLANEOUS DATA:

FL	- Lateral creep coefficient per wheel	= 3,000,000 lb.
FT	- Longitudinal creep coefficient per wheel	= 3,000,000 lb.
ZETA (ξ)		= 1.0
EPSI (ϵ)		= 0.05
RHO (δ)		= 0.05
XLAMD (λ)	- Effective conicity	= 0.05
W	- Axle load	= 65,000 lb.

TABLE 3

INPUT DATA FOR LS1 LOCOMOTIVE

DIMENSIONAL DATA:

A1	- Distance between truck center and lead axle	=	81.78 in.
A2	- Distance between truck center and middle axle	=	1.7136 in.
A3	- Distance between truck center and trailing axle	=	81.216 in.
B	- Half distance between wheel contact points	=	29.5 in.
B1	- Half lateral distance between primary suspension	=	39.756 in.
B2	- Half lateral distance between secondary suspension	=	35.496 in.
HT	- Height of truck frame center of gravity above axle center	=	4.878 in.
H1	- Height of bolster spring center above truck frame center of gravity	=	9.264 in.
H2	- Height of carbody center of gravity above bolster spring center	=	36.132 in.
HB	- Height of carbody center of gravity above axle center	=	50.274 in.
XL	- Half distance between truck centers	=	245.496 in.
RO	- Wheel tread radius	=	20.0 in.

MASS AND INERTIA DATA:

XMB	- Carbody Mass	=	779 lb.-sec. ² /in.
XMT	- Truck frame mass	=	37.6 lb.sec. ² /in.

TABLE 3 (Cont'd.)

MASS AND INERTIA DATA:

XMW	- Wheel set mass	=	34 lb.-sec. ² /in.
XIB	- Carbody yaw moment of inertia	=	35,300,000 lb.-in.-sec. ²
XJB	- Carbody roll moment of inertia	=	1,509,600 lb.-in.-sec. ²
XIT	- Truck frame yaw moment of inertia	=	161,424 lb.-in.-sec. ²
XJT	- Truck frame roll moment of inertia	=	52,656 lb.-in.-sec. ²
XIW	- Wheel set yaw moment of inertia	=	16,381.32 lb.-in.-sec. ²

SPRING RATES AND DAMPING DATA:

XKYW	- Lateral primary stiffness per axle	=	5,000 lb./in.
XKXW	- Longitudinal primary stiffness per axle	=	500,000 lb./in.
XKYT	- Lateral secondary stiffness per truck	=	8.400 lb./in.
XKYAT	- Yaw secondary stiffness per truck	=	10,583,714 lb.-in./rad.
XKJ	- Vertical primary stiffness per truck side	=	18,720 lb./in.
XKB	- Vertical secondary stiffness per truck side	=	112,667 lb./in.
CYW	- Lateral damping of axle	=	16.67 lb.-sec./in.
CXW	- Longitudinal damping of axle	=	16.67 lb.-sec./in.
CYT	- Lateral secondary damping per truck	=	50 lb.-sec./in.
CYAT	- Yaw Secondary damping per truck	=	63,000 lb.-in.-sec./rad.

TABLE 3 (Cont'd.)

SPRING RATES AND DAMPING DATA:

CJ	- Vertical primary damping per truck side	=	75 lb.-sec./in.
CB	- Vertical secondary damping per truck side	=	667 lb.-sec./in.

MISCELLANEOUS DATA:

FL	- Lateral creep coefficient $f = 3500 (dw)^{1/2}$	=	4,141,256 lb.
FT	- Longitudinal creep coefficient	=	4,141,256 lb.
ZETA (ξ)		=	1.0
EPSI (ϵ)		=	0.05
RHO (δ)		=	0.05
XLAMD (λ)	-Effective conicity	=	0.05
W	Axle load	=	70,000 lb.

TABLE 4

INPUT DATA FOR LS2 LOCOMOTIVE

DIMENSIONAL DATA:

A1	- Distance between truck center and lead axle	=	79.38 in.
A2	- Distance between truck center and middle axle	=	- 1.25 in.
A3	- Distance between truck center and trailing axle	=	85.0 in.
B	- Half distance between wheel contact points	=	29.5 in.
B1	- Half lateral distance between primary suspension	=	39.5 in.
B2	- Half lateral distance between secondary suspension	=	35.12 in.
HT	- Height of truck frame center of gravity above axle center	=	2.5 in.
H1	- Height of bolster spring center above truck frame center of gravity	=	5.0 in.
H2	- Height of carbody center of gravity above bolster spring center	=	50.2 in.
HB	- Height of carbody center of gravity above axle center	=	57.70 in.
XL	- Half distance between truck centers	=	276.0 in.
RO	- Wheel tread radius	=	20.0 in.

MASS AND INERTIA DATA:

XMB	- Carbody mass	=	766 lb.-sec. ² /in.
XMT	- Truck frame mass	=	40.0 lb.-sec. ² /in.

TABLE 4 (Cont'd.)

MASS AND INERTIA DATA:

XMW	- Wheel set mass	=	30.0 lb.-sec. ² /in.
XIB	- Carbody yaw moment of inertia	=	39,600,000 lb.-in.-sec. ²
XJB	- Carbody roll moment of inertia	=	1,720,000 lb.-in.-sec. ²
XIT	- Truck frame yaw moment of inertia	=	178,000 lb.-in.-sec. ²
XJT	- Truck frame roll moment of inertia	=	56,000 lb.-in.-sec. ²
XIW	- Wheel set yaw moment of inertia	=	16,500 lb.-in.-sec. ²

SPRING RATES AND DAMPING DATA:

XKYW	- Lateral primary stiffness per axle	=	5,000 lb./in.
XKXW	- Longitudinal primary stiffness per axle	=	500,000 lb./in.
XKYT	- Lateral secondary stiffness	=	22,000 lb./in.
XKYAT	- Yaw secondary stiffness per truck	=	10,000,000 lb.-in./rad.
XKJ	- Vertical primary stiffness per truck	=	19,800 lb./in.
XKB	- Vertical secondary stiffness per truck side	=	250,000 lb./in.
CYW	- Lateral damping of axle	=	400 lb.-sec./in.
CXW	- Longitudinal damping of axle	=	12.5 lb.-sec./in.
CYT	- Lateral secondary damping per truck	=	600 lb.-sec./in.

TABLE 4 (Cont'd.)

SPRING RATES AND DAMPING DATA:

CYAT	- Yaw secondary damping per truck	=	200,000 lb.-in.-sec./rad.
CJ	- Vertical primary damping per truck side	=	150 lb.-sec./in.
CB	- Vertical secondary damping per truck side	=	250 lb.-sec./in.

MISCELLANEOUS DATA:

FL	- Lateral creep coefficient	4,000,000 lb.
FT	- Longitudinal creep coefficient	4,000,000 lb.
ZETA (ξ)		1.0
EPSI (ϵ)		0.05
RHO (δ)		0.05
XLAMD (λ)	- Effective	0.05
W	- Axle Load	66,000 lb.

TABLE 5

SUMMARY OF PARAMETRIC STUDY OF LS2 LOCOMOTIVE

<u>DESCRIPTION</u>	<u>CRITICAL SPEED - MPH</u>	<u>PERCENTAGE CHANGE FROM BASIC</u>
Basic Locomotive	121.5	
Lateral Stiffness of Axle, 7,000 Lb./In., i.e. 140% of Base Value	139.0	14.4
Effective Wheel Taper, 1 in 10 (Base Value is 1 in 20)	83.0	31.7
Lateral Primary Damping, 600 Lb.-Sec./In., i.e. 150% of Base Value	128	5.3
Lateral Secondary Damping	- No Change in Critical Speed -	
Mass and Roll Moment of Inertia	- No Change in Critical Speed -	
Yaw Moment of Inertia of the Carbody 150% of Base Value	119.5	1.6
Mass and Roll Moment of Inertia of the Truck Frame	- No Change in Critical Speed -	
Yaw Moment of Inertia of the Truck Frame 150% of Base Value	106	12.8
Yaw Moment of Inertia of the Wheel Set 150% of Base Value	116	4.5
Tangential Creep Coefficient per Wheel 150% of Base Value	109	10.3
Lateral Creep Coefficient per Wheel 150% of Base Value	128	5.3

SUMMARY OF PARAMETER

<u>Parameter Description</u>	<u>Value</u>	<u>(% Base)</u>
Basic Locomotive		
Half length of wheel base (inches)	48 60	(89%) (111%)
Height of Body above the axle (inches)	41 81	(68%) (132%)
Half distance between Truck Centers (inches)	154 254	(75%) (125%)
69 Wheel tread Radius (in.)	15 25	(75%) (125%)
Mass of the Body (lb.)	273 819	(50%) (150%)
Mass of the Truck (lb.)	9.7 29.1	(50%) (150%)
Moment of inertia of the Body in Yaw (10^6 lb. in. sec ²)	9.9 29.7	(50%) (150%)
Moment of inertia of the Body in Yaw (lb.in.sec ²)	10,000 30,000	(50%) (150%)

TABLE 6

EMPIRIC STUDY OF LFL LOCOMOTIVE

<u>Lower Bound of Primary Hunting Velocity (% Base)</u>	<u>Upper Bound of Primary Hunting Velocity (% Base)</u>	<u>Secondary Hunting Velocity (% Base)</u>
28.7	38.1	139.2
22.8 (79%) stable	39.9 (105%) stable	123.4 (89%) 156.4 (112%)
- No change	from basic	Locomotive -
- No change	from basic	Locomotive -
18.2 (63%) stable	47.0 (123%) stable	- No change - - No change -
19.9 (69%)	26.9 (71%)	118.6 (85%)
29.5 (103%)	56.3 (148%)	158.2 (114%)
		- No change - - No change -
		149.1 (107%) 128.6 (92%)
stable	stable	- No change -
19.9 (69%)	44.2 (116%)	- No change -
- No change	-	146.3 (105%)
- No change	-	133.0 (95%)

Moment of inertia of the Wheel-axle set in	6,000	(50%)
Yaw (lb.in.sec ²)	18,000	(150%)
Moment of inertia of the Body in	5.85	(50%)
Roll (10 ⁶ lb.in.sec. ²)	17.55	(150%)
Moment of inertia of of the Truck in	4,060	(50%)
Roll (lb.in.sec. ²)	12,180	(150%)
Lateral Stiffness of the Axle (lb/in.)	4,000 12,000	(50%) (150%)
Vertical Rate of the Bolster spring per truck side (lb/in.)	5,650 16,950	(50%) (150%)
Vertical Rate of the Journal spring per truck side (lb/in.)	8,076 24,228	(50%) (150%)
Effective Wheel Taper	.025 .100 .150	(50%) (200%) (300%)
Trngential Creep Coefficient per Wheel(10 ⁶ lb.)	1.5 4.5	(50%) (150%)
Lateral Creep Coefficient per Wheel (10 ⁶ lb.)	1.5 4.5	(50%) (150%)

TABLE 6 (Cont'd)

- No	change	-	148.0	(106%)
- No	change	-	131.7	(95%)
			- No change -	
			- No change -	
			- No change -	
			- No change -	
			97.8	(70%)
			181.5	(130%)
			- No change -	
			- No change -	
			- No change -	
			- No change -	
39.3	(137%)	177.8	(466%)	210.8 (151%)
	stable		stable	95.3 (68%)
	stable		stable	76.9 (55%)
	stable		stable	177.6 (127%)
19.7	(69%)	39.9	(105%)	121.6 (87%)
22.1	(77%)	127.0	(334%)	117.6 (84%)
	stable		stable	149.2 (107%)

TABLE 6 (Cont'd)

Longitudinal damping of the Axle (lb.sec./in.)	100	(Base = 0)	24.3	(85%)	38.4	(101%)	- No change -
Lateral damping of the Axle (lb.sec./in.)	100	(Base = 0)	stable		stable		- No change -
Lateral damping of the Truck (lb.sec./in.)	100	(100%)	stable		stable	146.6	(105%)
{ Lateral damping of the Truck (lb.sec./in.) and Effective Wheel Taper	100	(100%)	stable		stable	226.4	(163%)

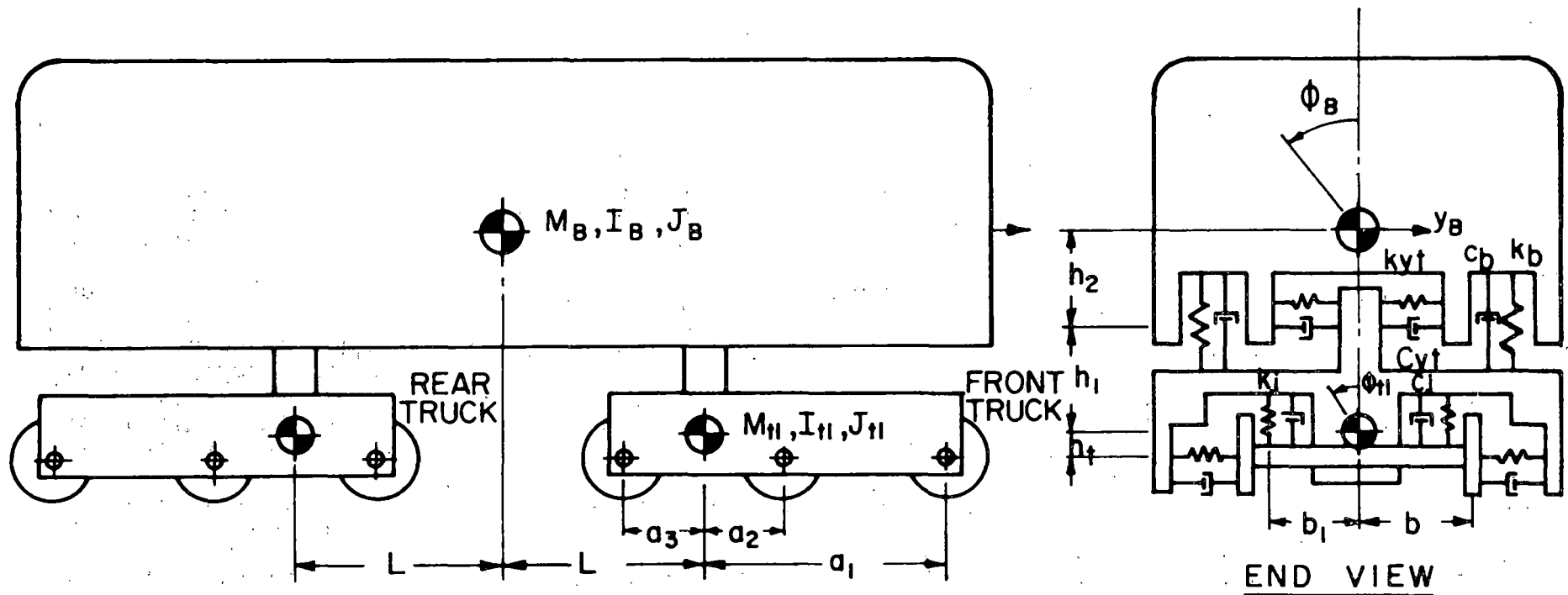
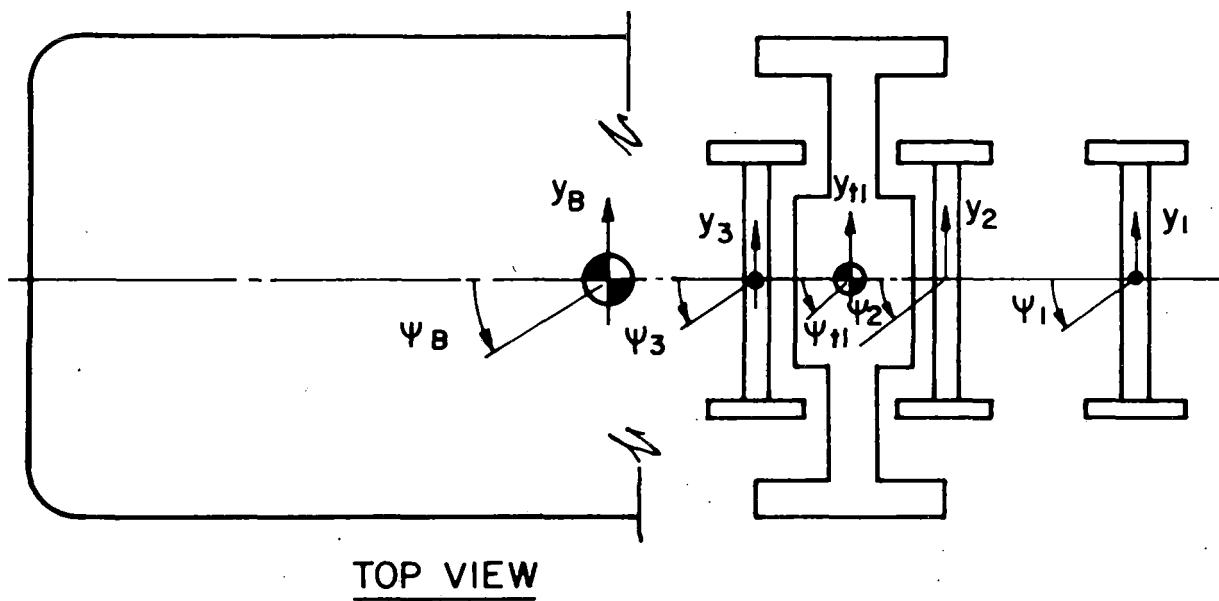


FIG. 1 VEHICLE MODEL - 6 AXLE LOCOMOTIVE

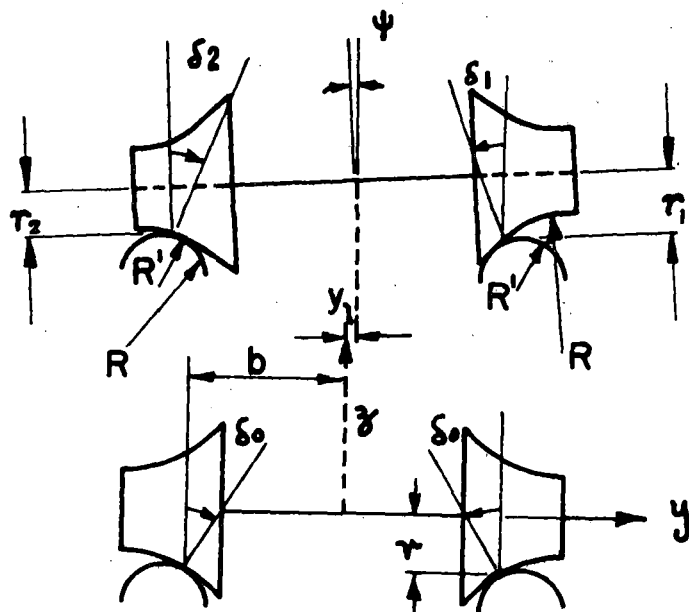


FIG. 2 WHEEL SET DISPLACED

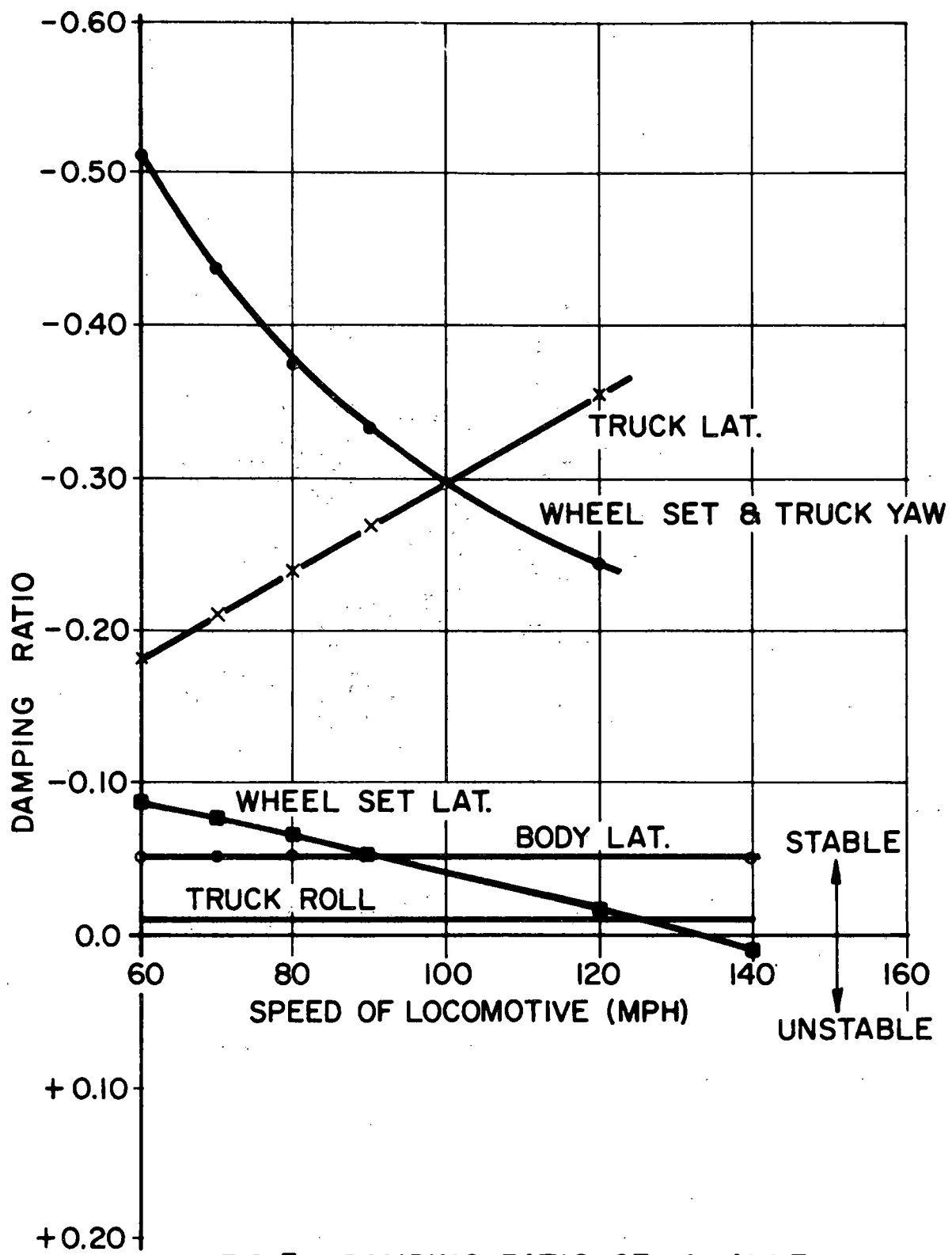


FIG. 3 DAMPING RATIO OF 4-AXLE VEHICLE (ACT I) OSCILLATIONS

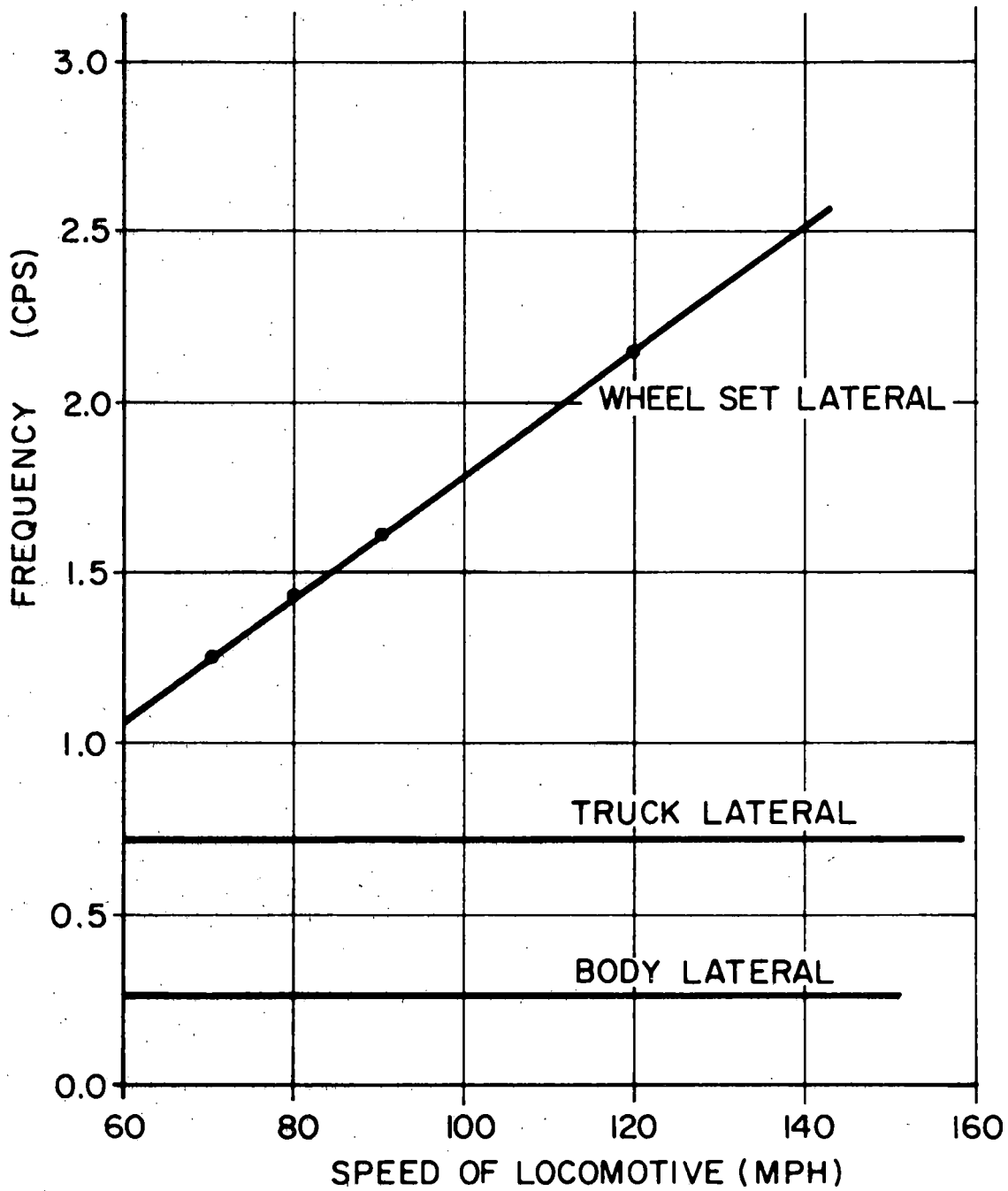


FIG. 4 CHARACTERISTIC FREQUENCIES OF
ACT 1 VEHICLE

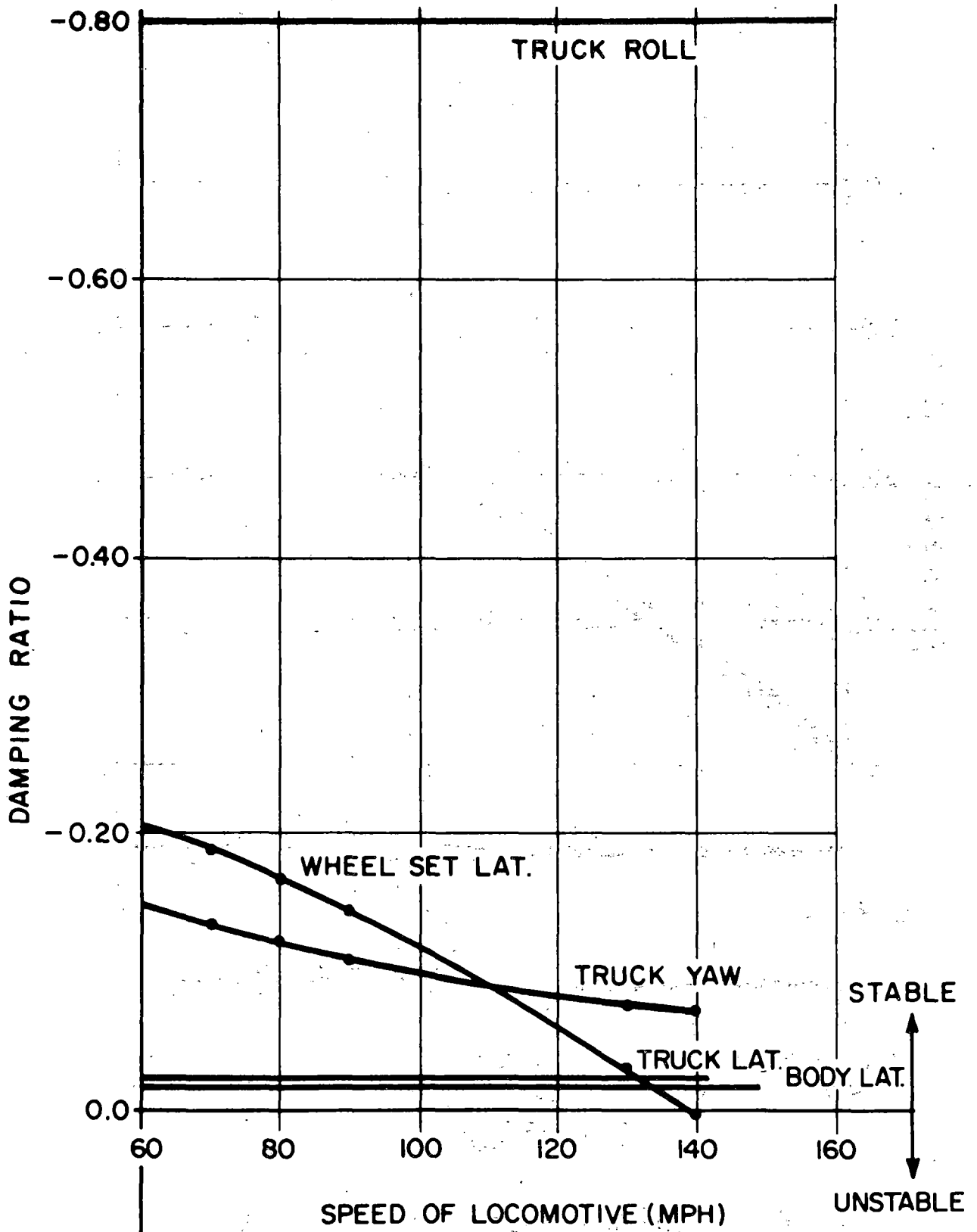


FIG. 5 DAMPING RATIO OF 4-AXLE LOCOMOTIVE (LF 1) OSCILLATIONS

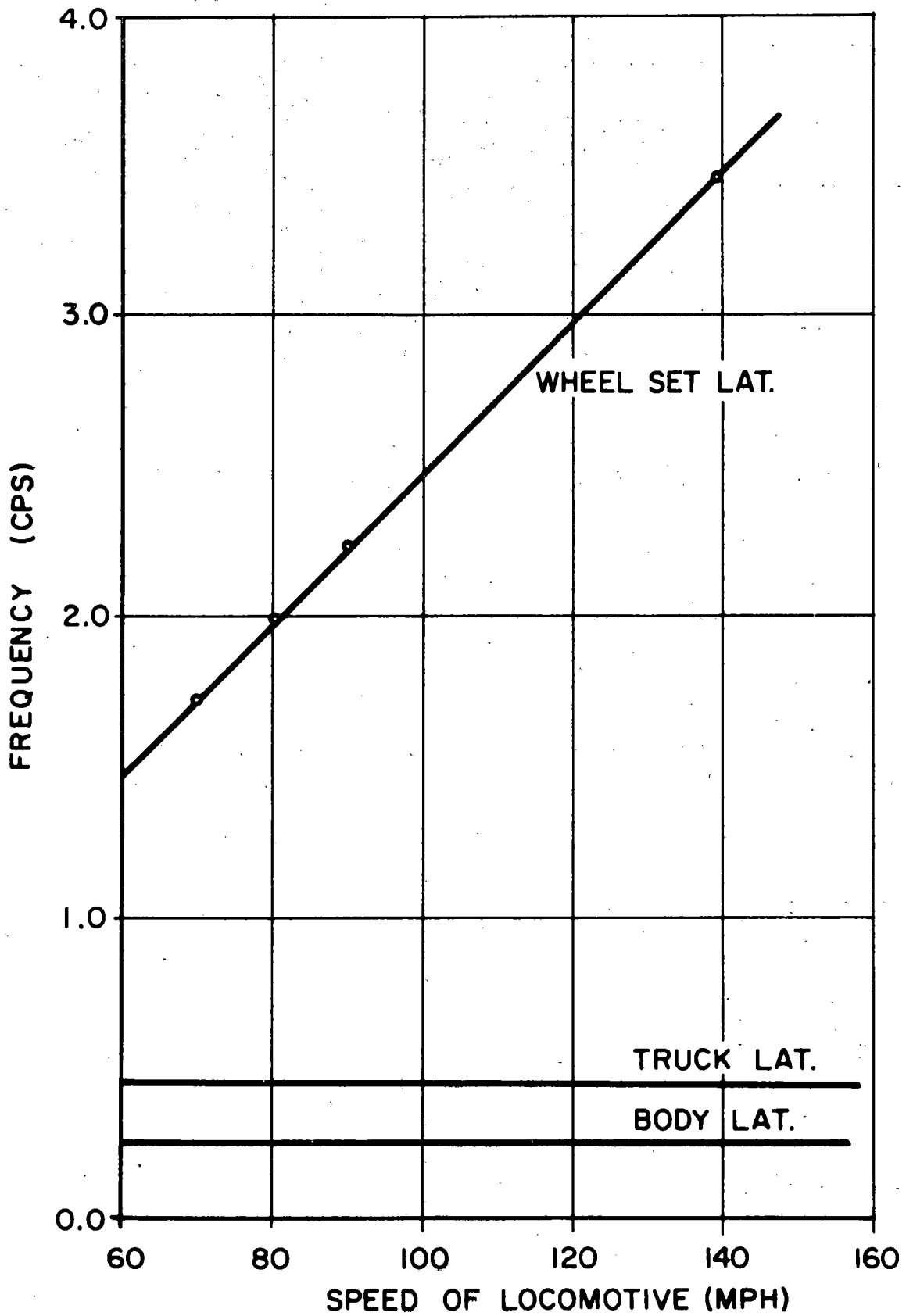


FIG.6 CHARACTERISTIC FREQ. OF LF 1 LOCOMOTIVE

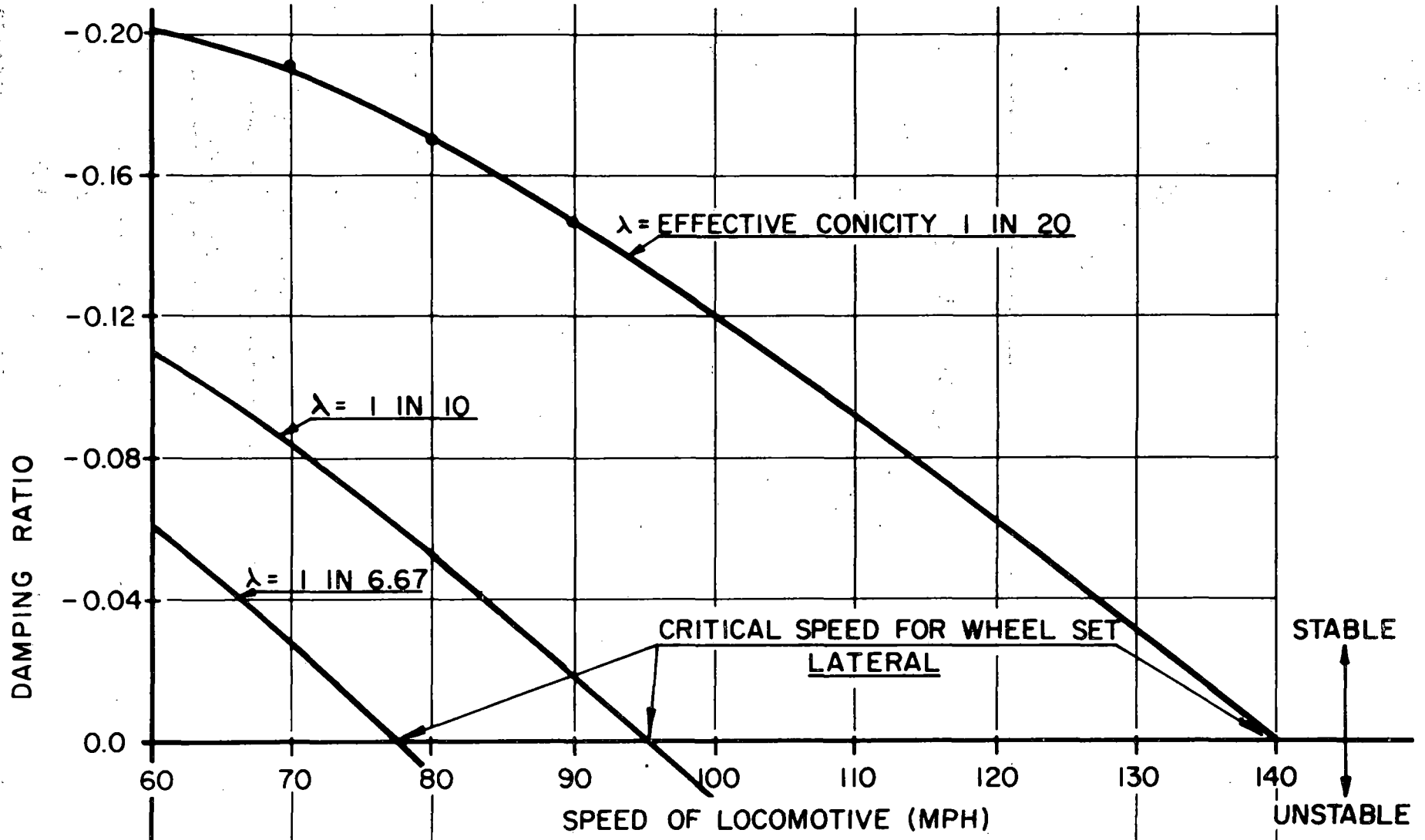


FIG.7 CRITICAL SPEED VS EFFECTIVE CONICITY FOR LF 1

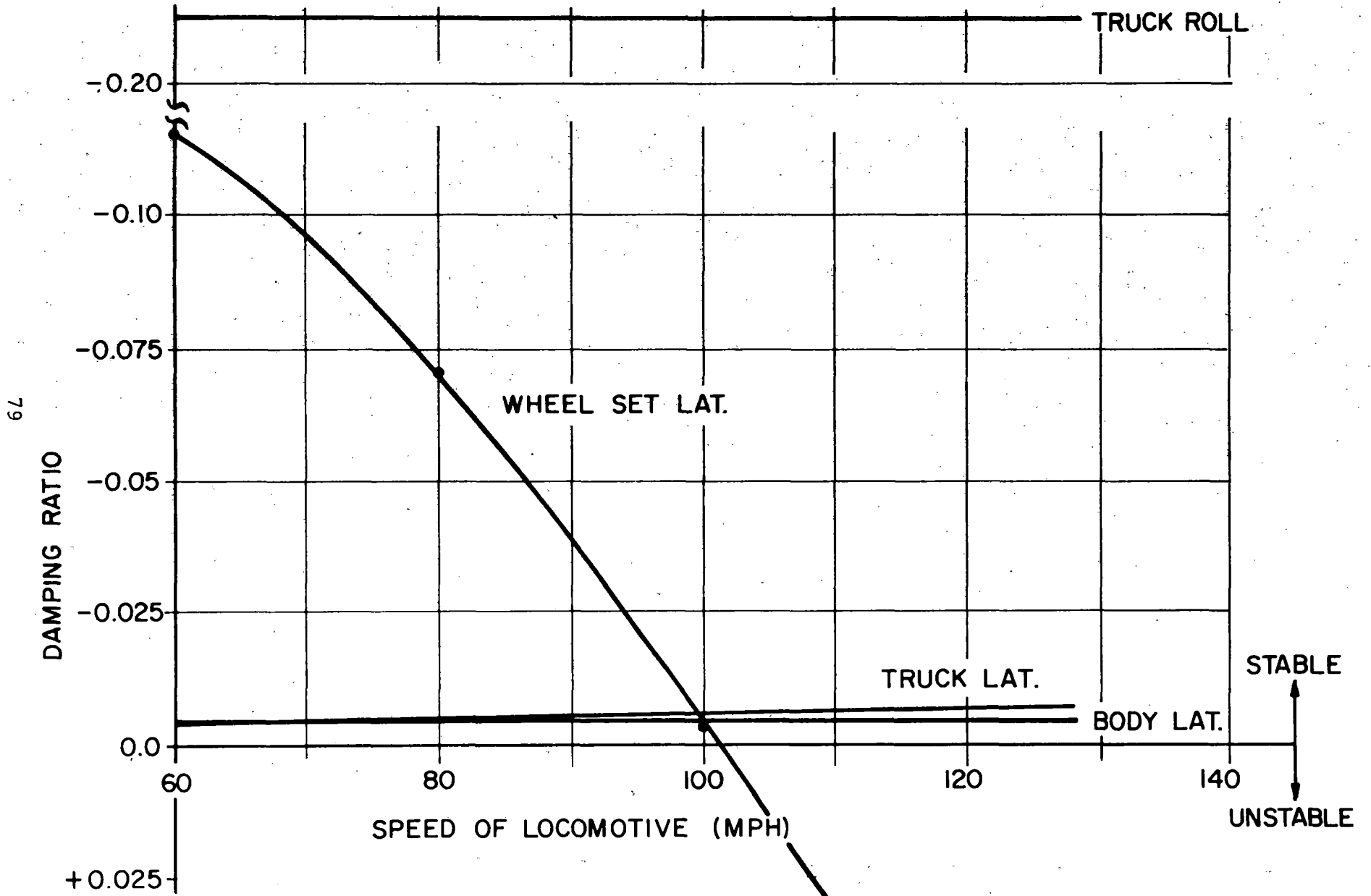


FIG. 8 DAMPING RATIO OF 6-AXLE LOCOMOTIVE (LS 1) OSCILLATIONS

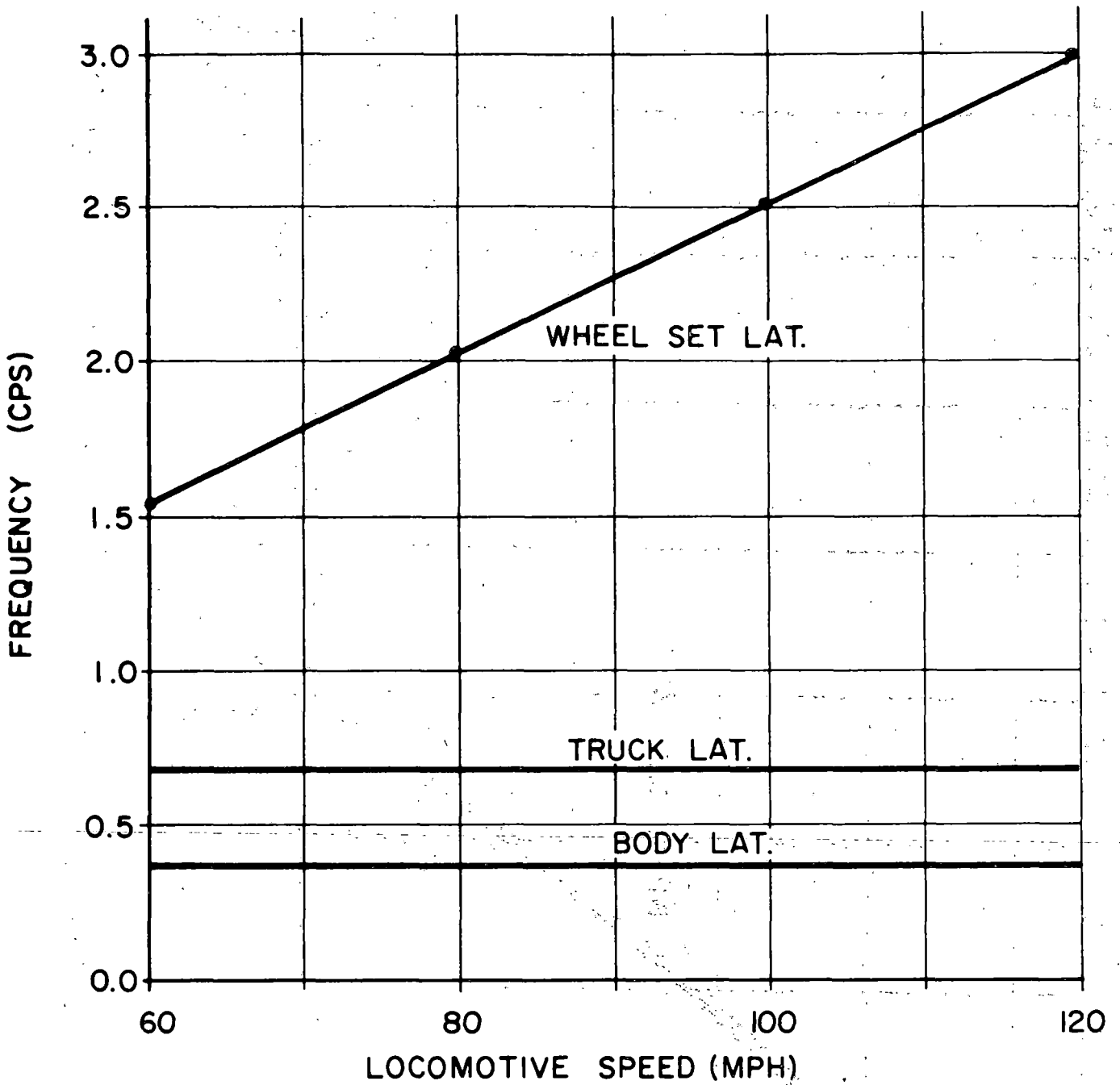


FIG.9 CHARACTERISTIC FREQUENCIES OF
6-AXLE LS 1 LOCOMOTIVE

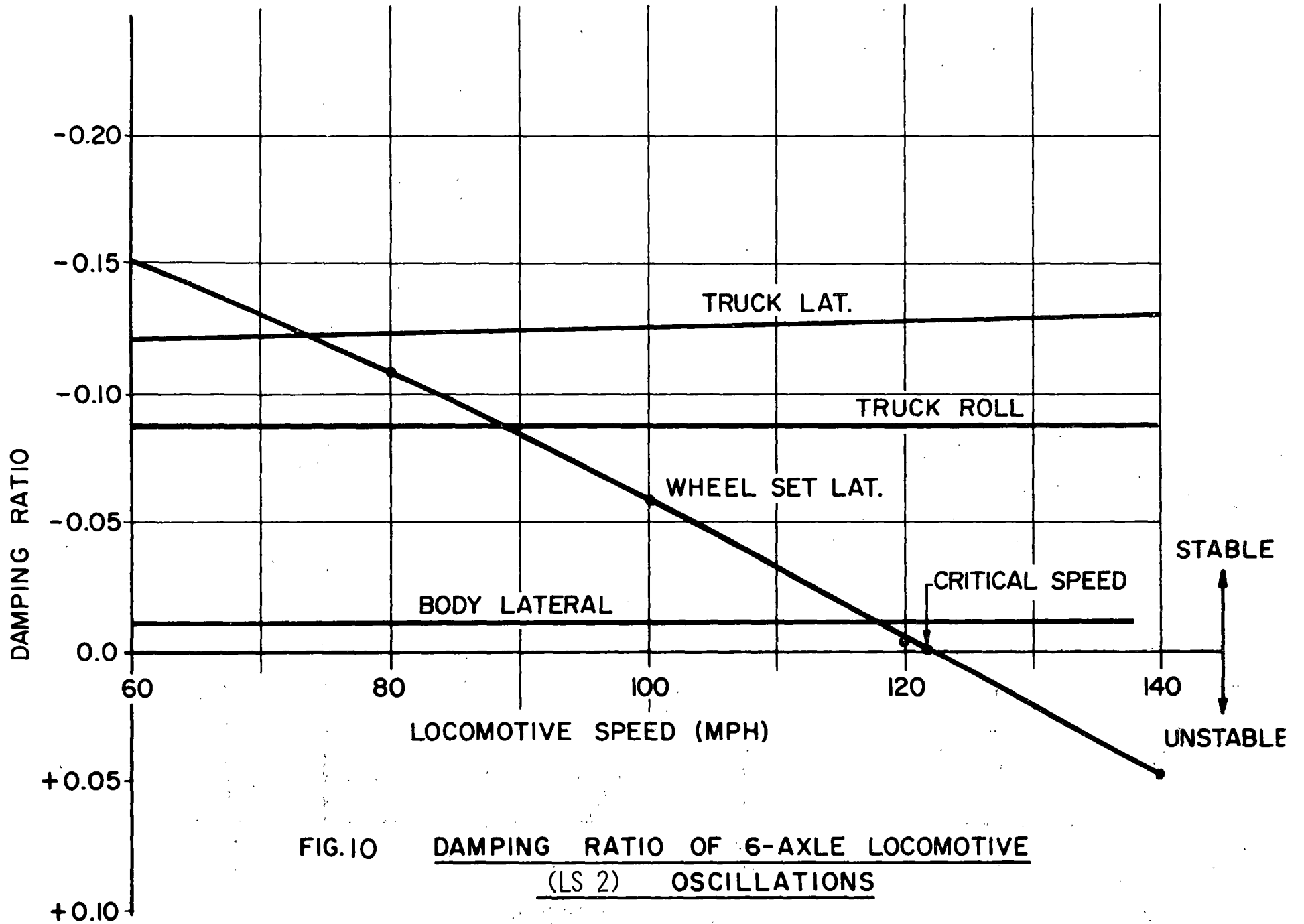


FIG. 10 DAMPING RATIO OF 6-AXLE LOCOMOTIVE
(LS 2) OSCILLATIONS

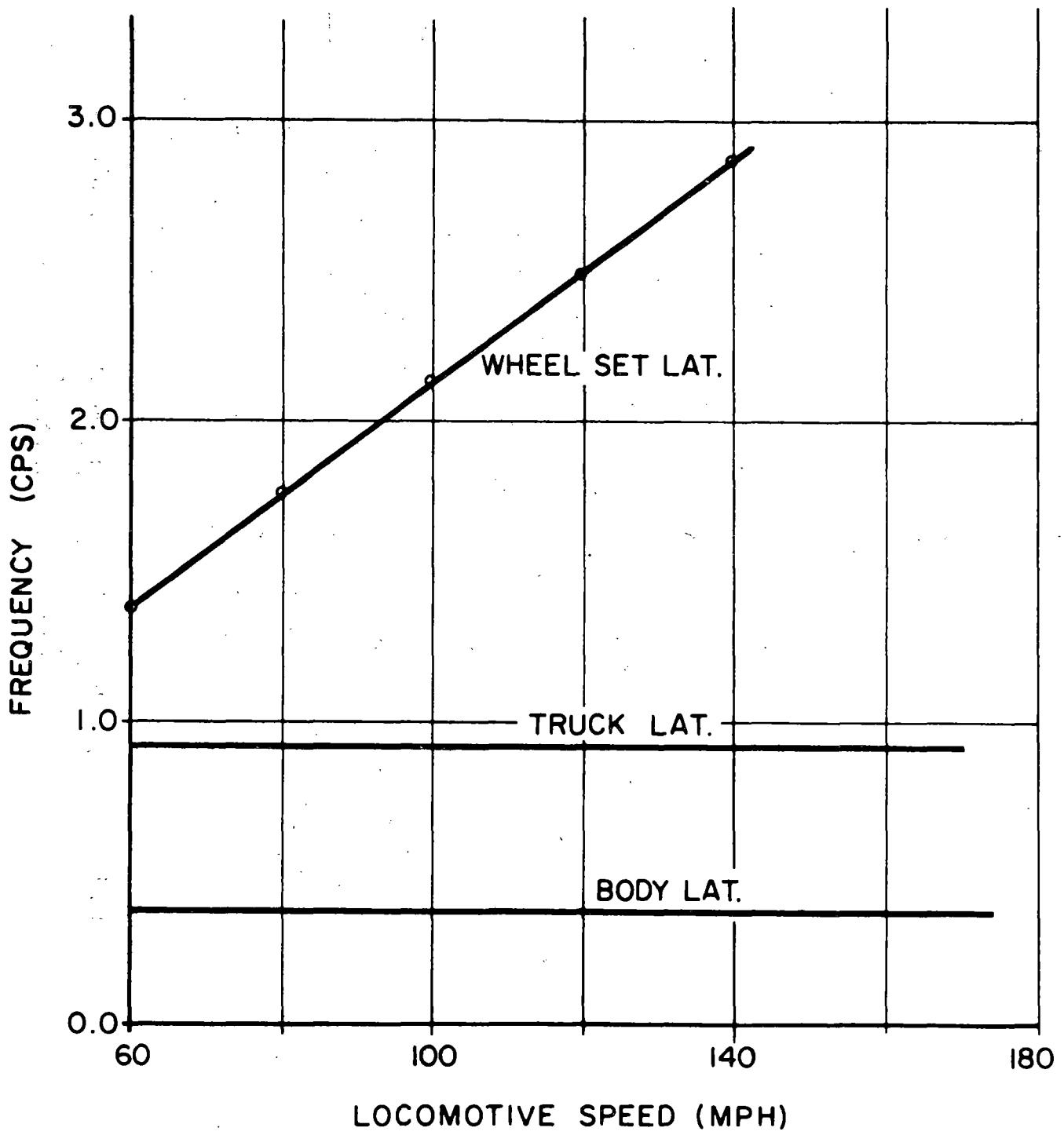


FIG. II CHARACTERISTIC FREQUENCIES OF
LS 2 LOCOMOTIVE

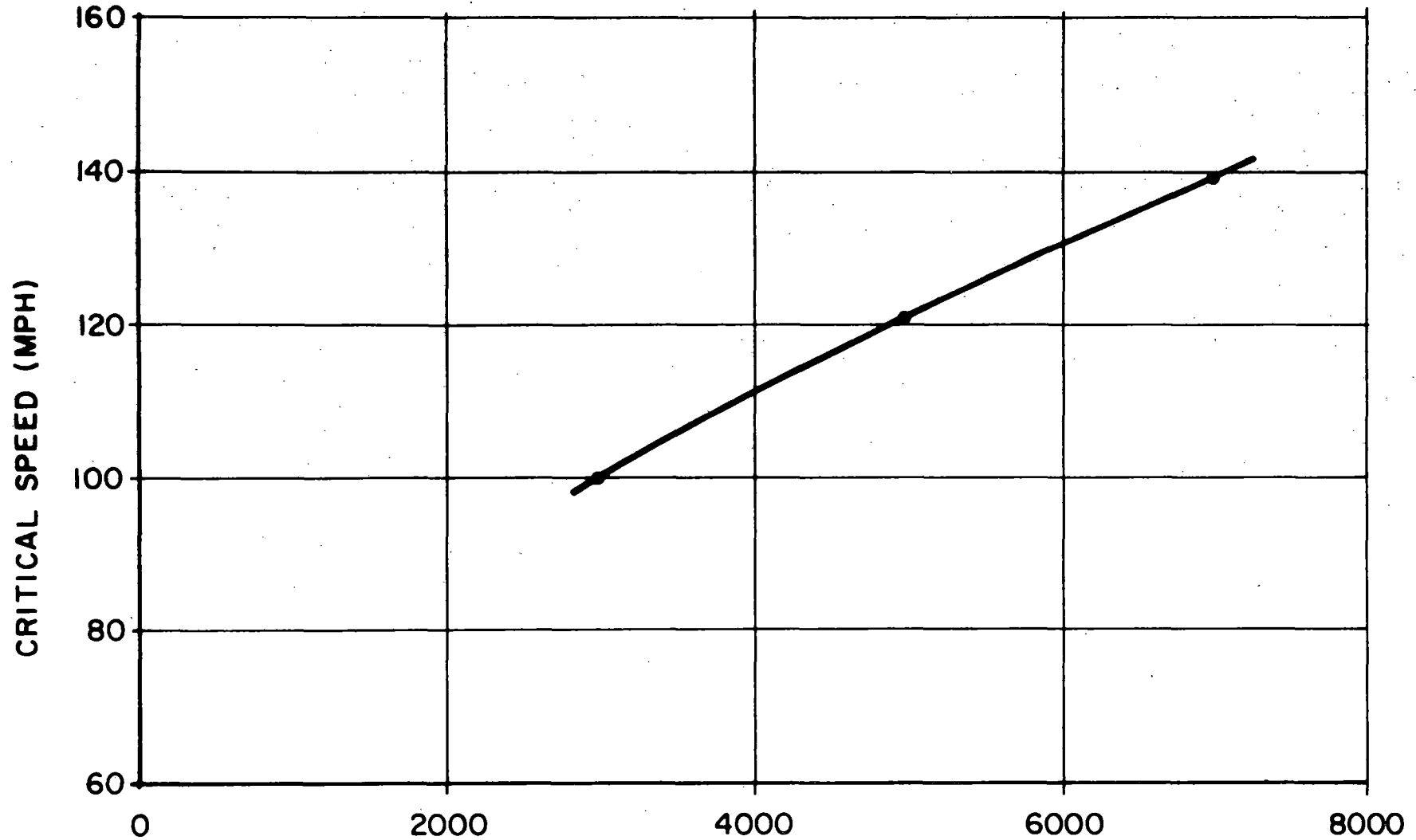


FIG. 12 CRITICAL SPEED VS LATERAL STIFFNESS OF
PRIMARY SUSPENSION FOR LS 2 LOCOMOTIVE

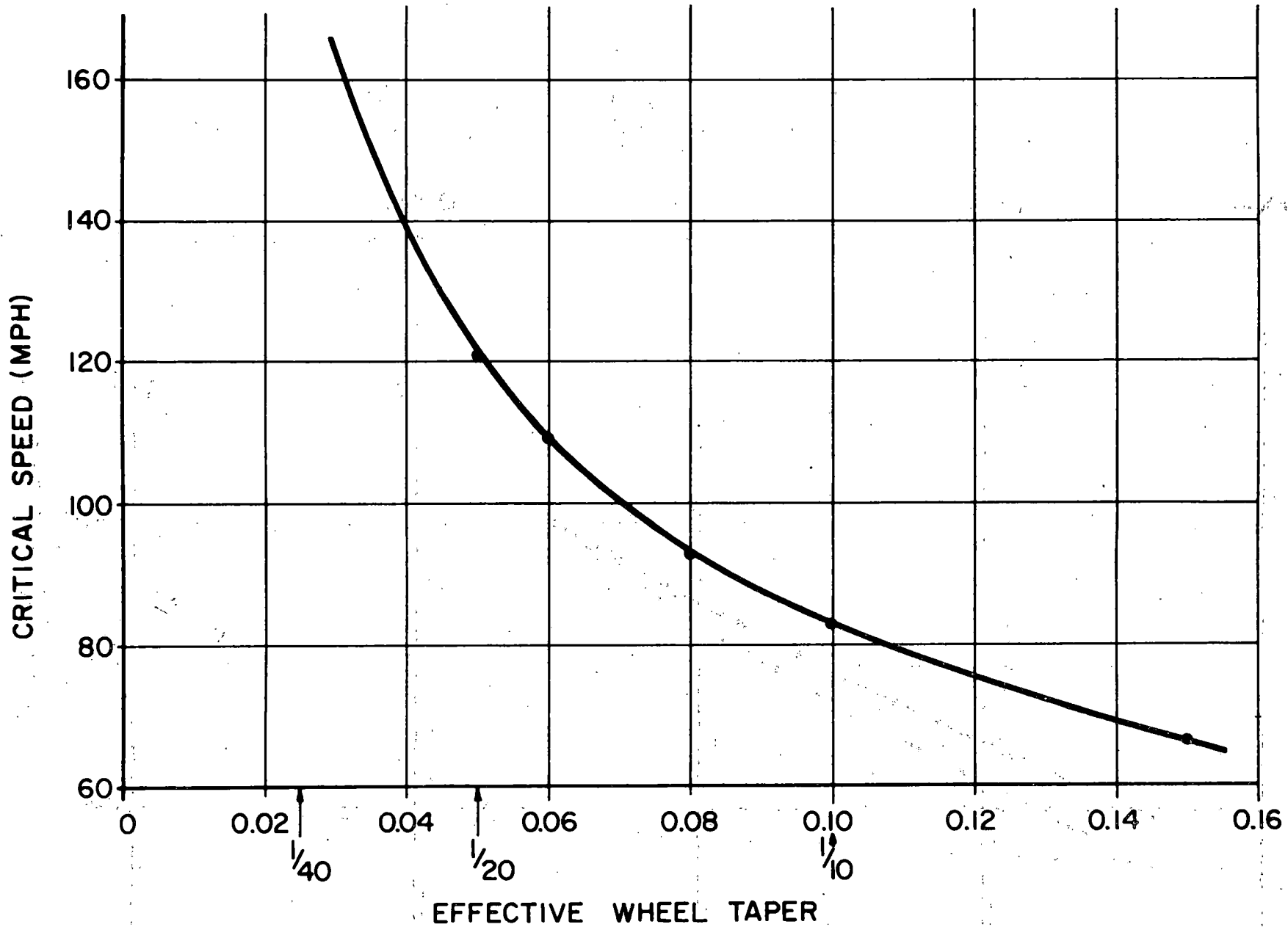


FIG. 13

CRITICAL SPEED VS EFFECTIVE WHEEL TAPER
FOR LS 2 LOCOMOTIVE

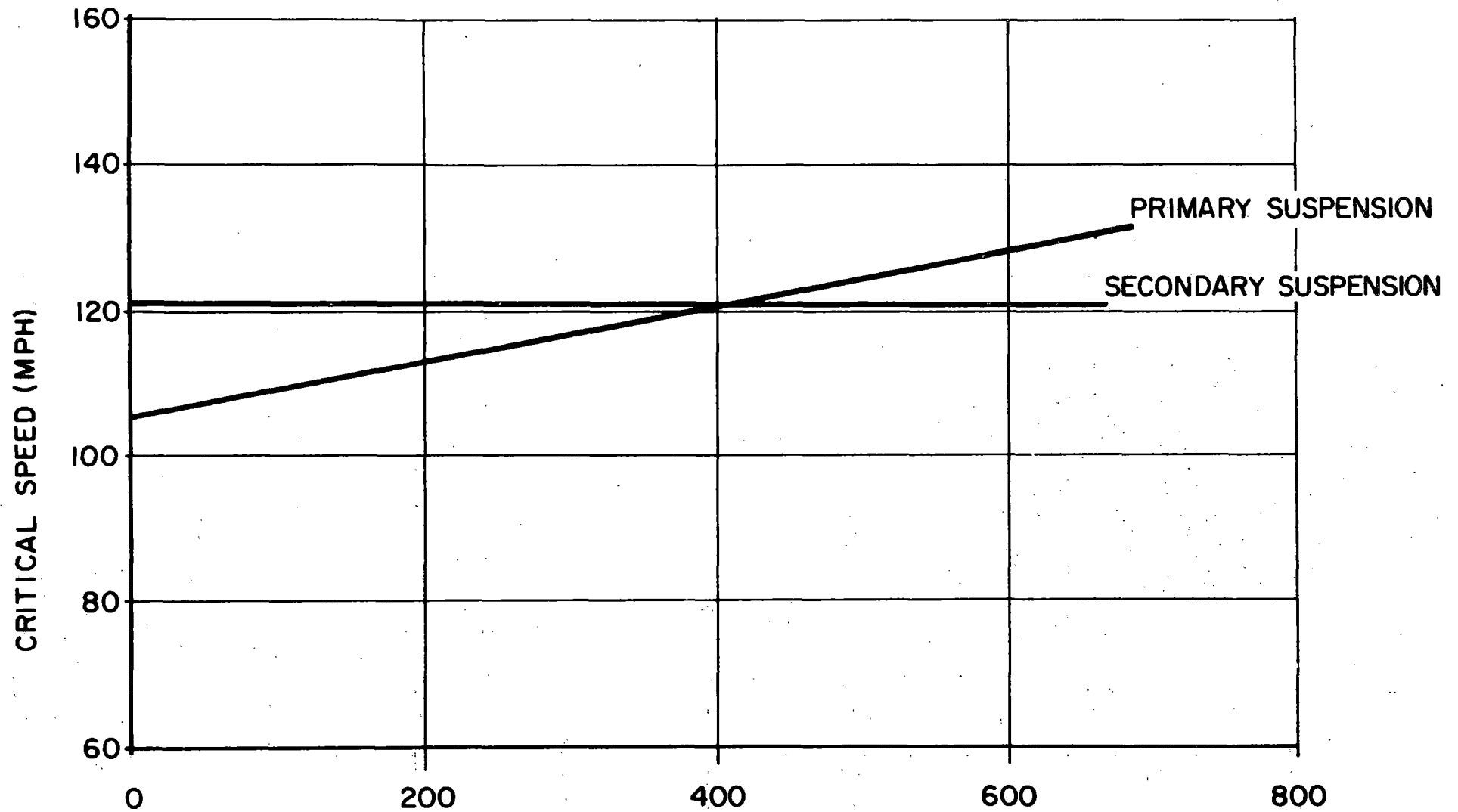


FIG. 14 CRITICAL SPEED VS LATERAL DAMPING FOR
LS 2 LOCOMOTIVE

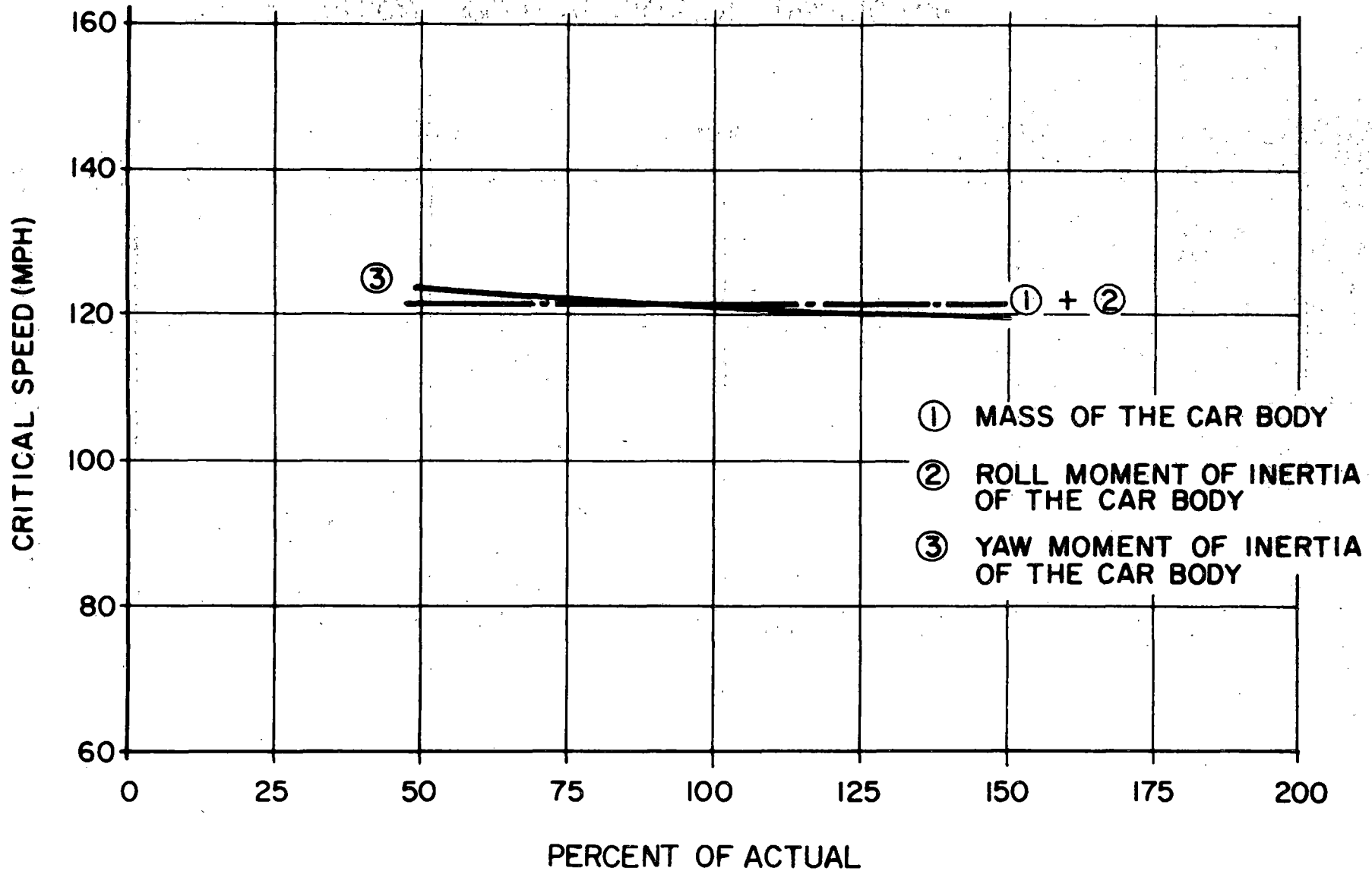


FIG. 15 CRITICAL SPEED VS CARBODY MASS AND MOMENT OF INERTIAS FOR LS 2 LOCOMOTIVE

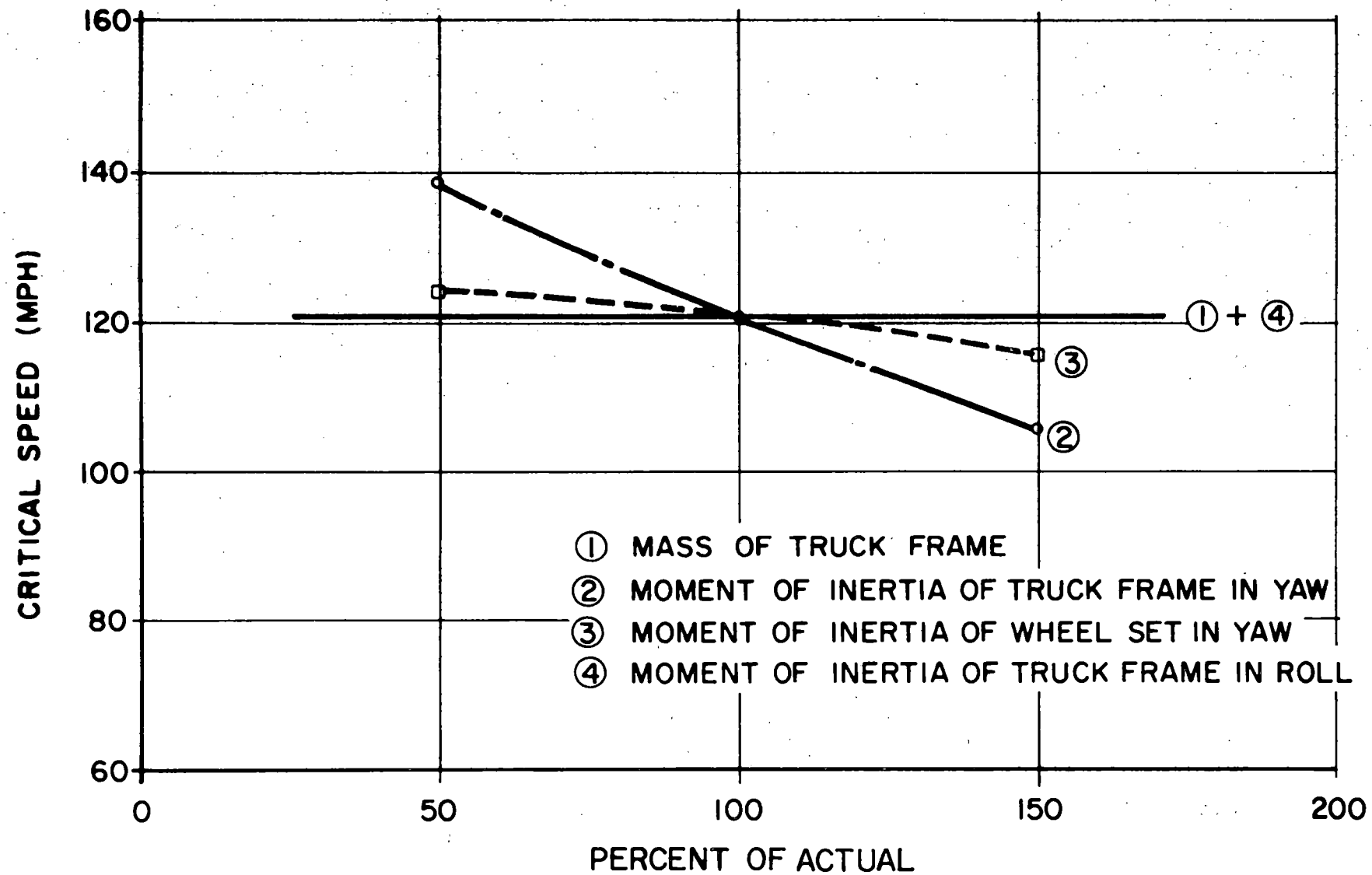


FIG. 16 CRITICAL SPEED VS TRUCK FRAME MASS AND
MOMENT OF INERTIAS FOR : LS 2 LOCO

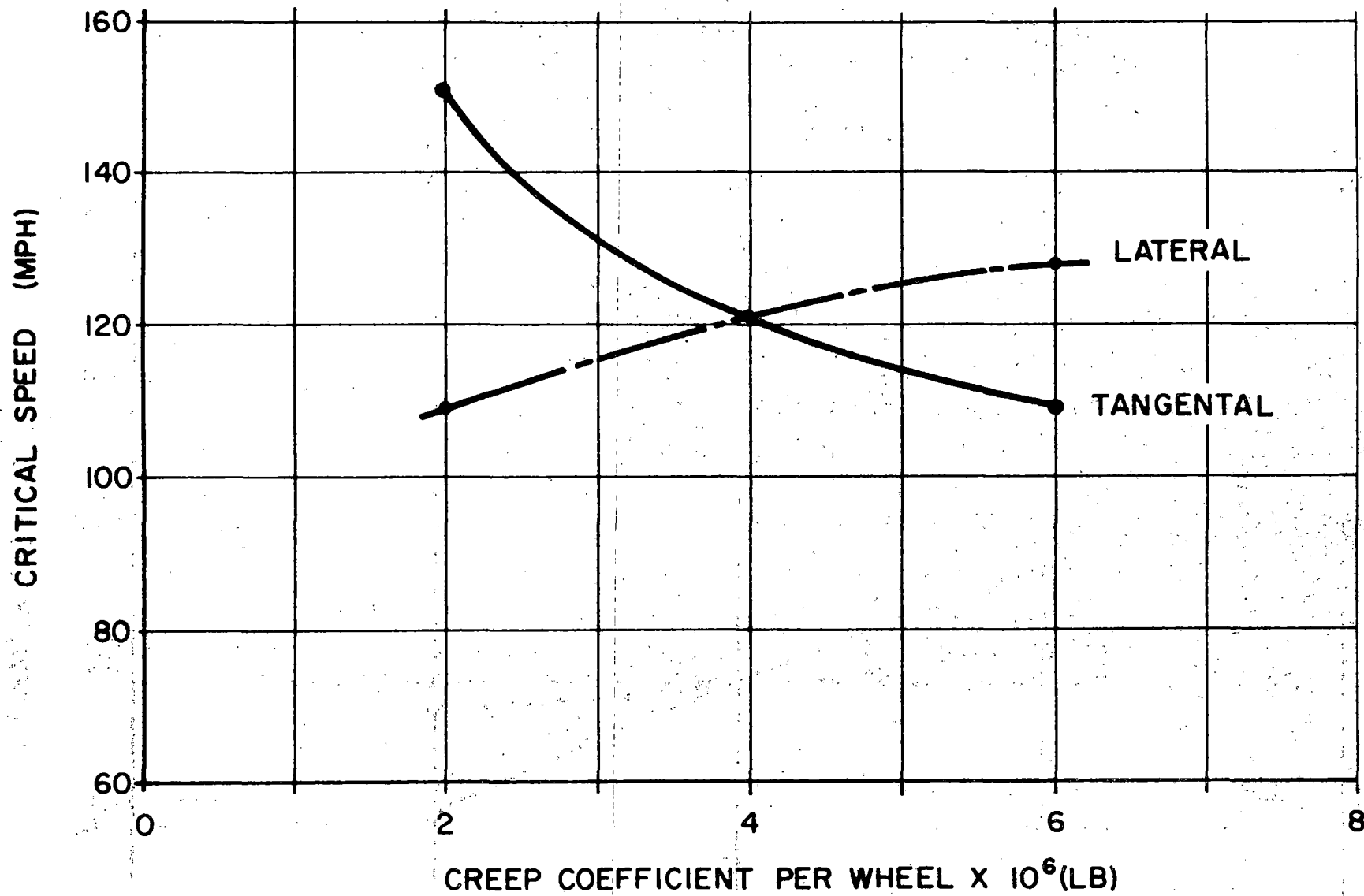


FIG.17 CRITICAL SPEED VS CREEP COEFFICIENT FOR
LS 2 LOCOMOTIVE

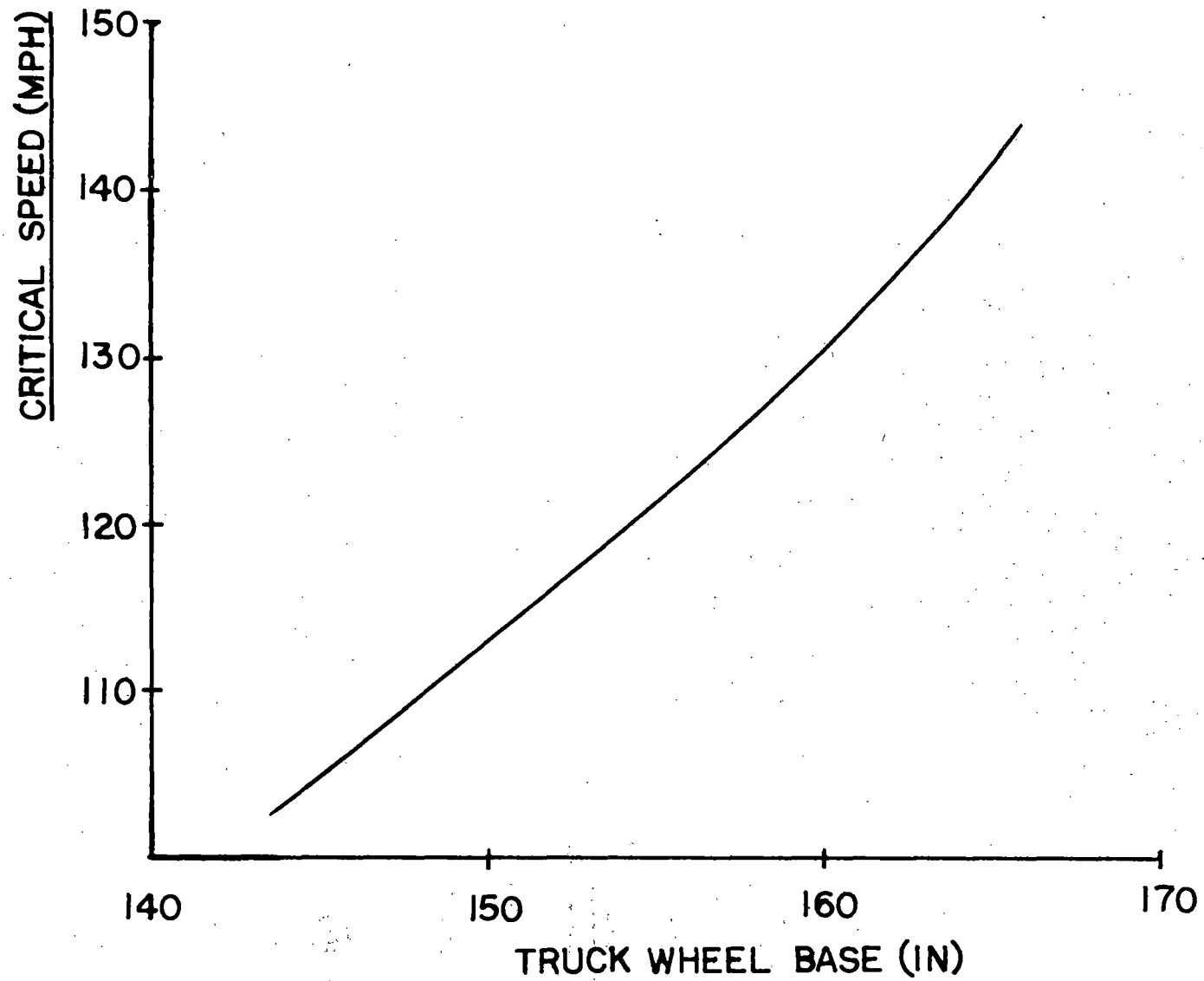


FIG. 18 CRITICAL SPEED VS TRUCK WHEEL BASE
FOR LS 2 LOCOMOTIVE

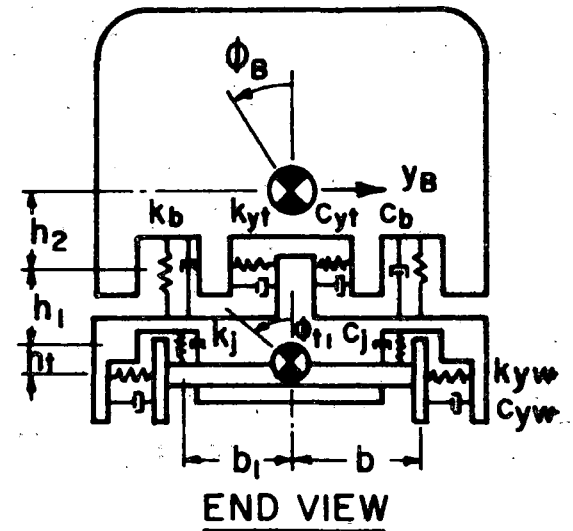
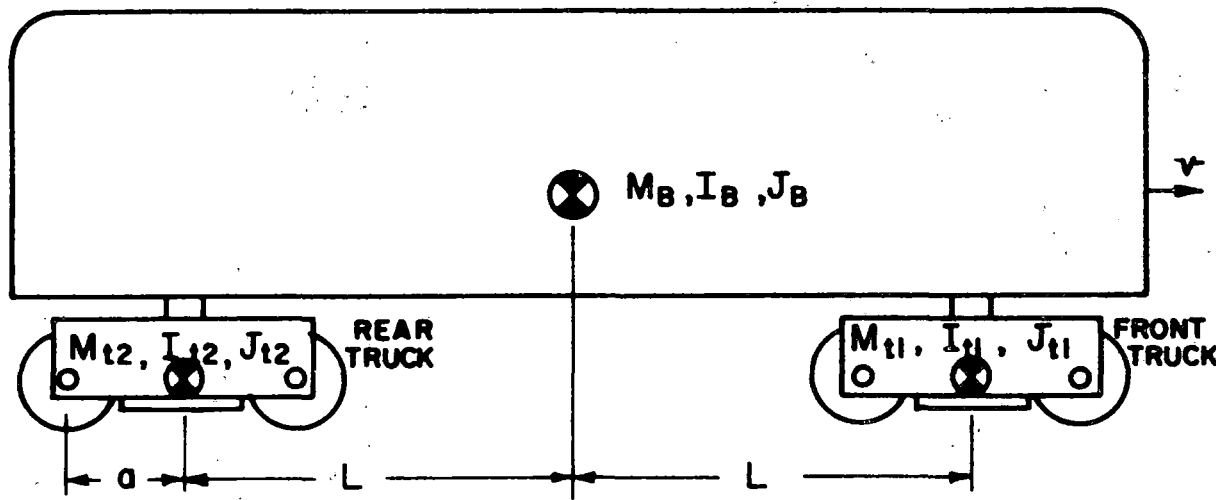
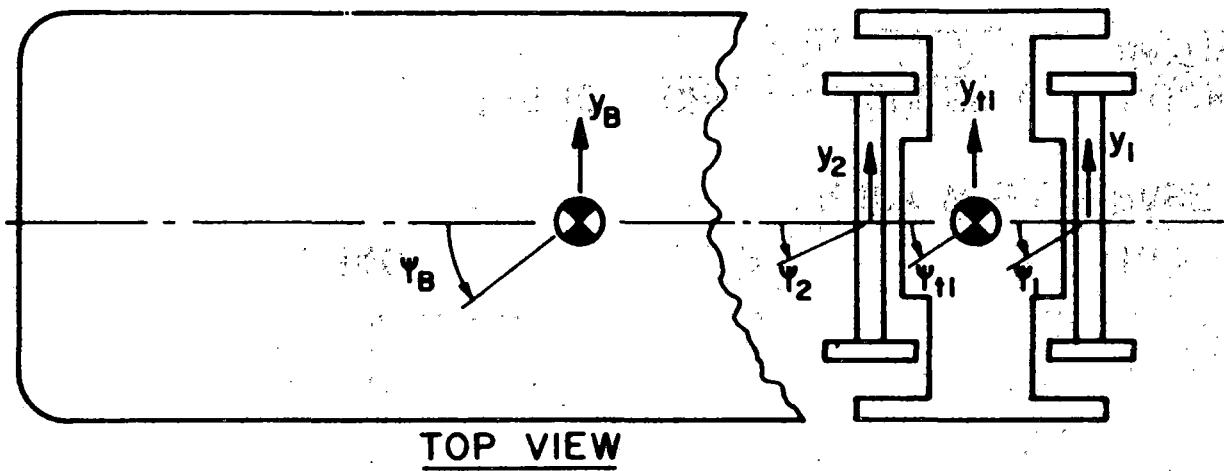


FIG. B-1 VEHICLE MODEL 4-AXLE LOCOMOTIVE

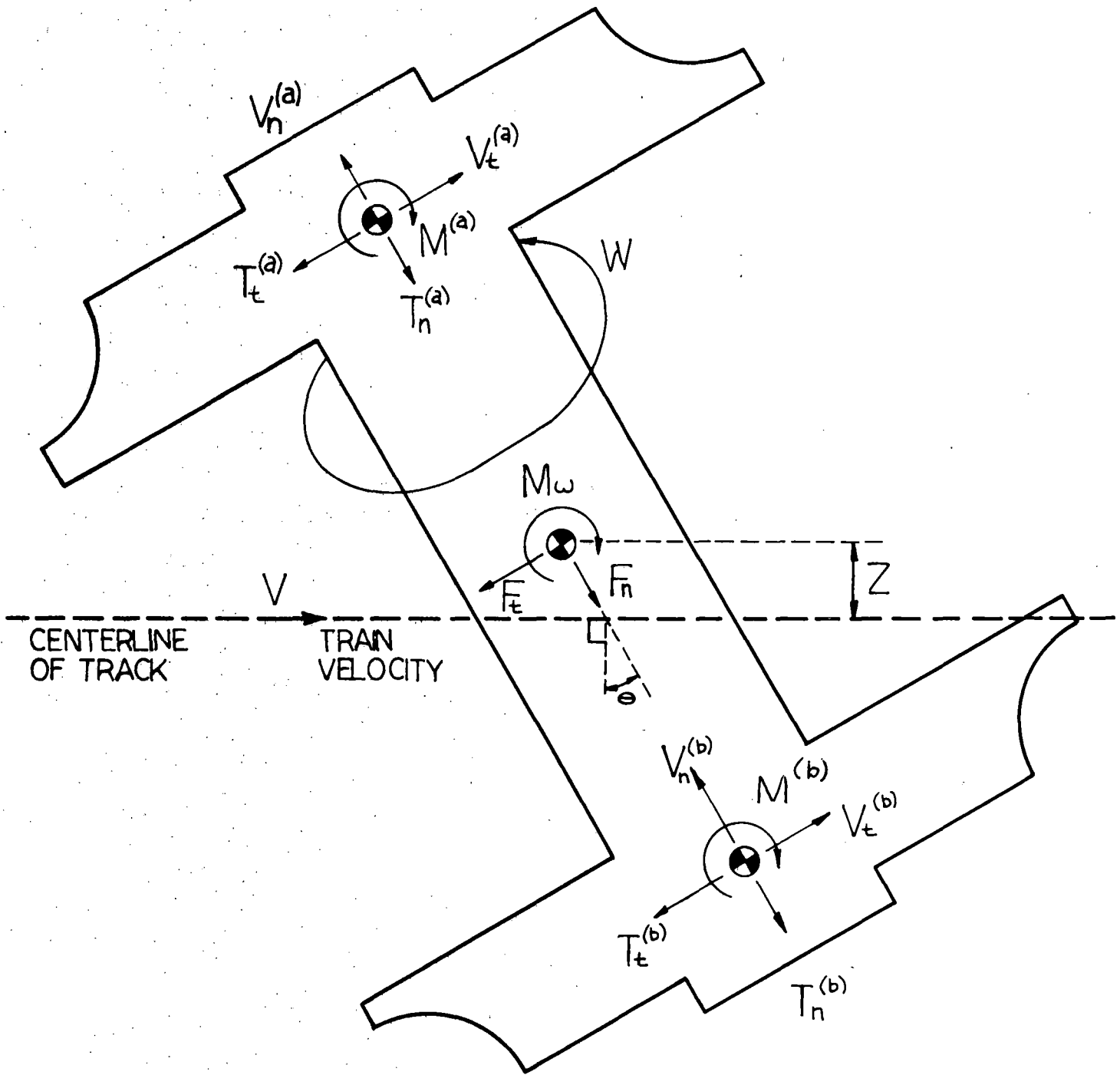


FIG. B-2 CREEP

PROPERTY OF FRA
RESEARCH & DEVELOPMENT
LIBRARY

Locomotive Truck Hunting Model, Technical
Documentation.
VK Garg, GC Martin, PW Hartman, JG Tolomei